Energy Conversion and Management: X 31 (2026) 102186

Contents lists available at ScienceDirect

Energy Conversion and Management: X

journal homepage: www.sciencedirect.com/journal/energy-conversion-and-management-x

Subhourly temporal resolution in PV energy system modeling: effects on design, reliability, and computational efficiency

Olalekan Omoyele [a,b,*], Maximilian Hoffmann [a], Jann Michael Weinand [a], Detlef Stolten [a,b]

[a] Forschungszentrum Jülich GmbH, Institute of Climate and Energy Systems, Jülich Systems Analysis (ICE-2), 52425 Jülich, Germany
[b] RWTH Aachen University, Faculty of Mechanical Engineering, 52062 Aachen, Germany

ARTICLE INFO

Keywords:
Temporal resolution
Time series aggregation
Renewable energy systems
Microgrids
Self-sufficiency
Optimization

ABSTRACT

The shift toward high temporal resolution modeling of energy systems is crucial due to the growing reliance on intermittent renewable energy sources. Hourly data has traditionally been used, but it lacks the temporal detail required to accurately capture total system costs, component sizing, operational feasibility, and reliability. This study investigates the impact of minute-resolution on the design and optimization of photovoltaic-based energy systems at both single- and aggregated-building levels, represented by a self-sufficient building and a microgrid, respectively. The objective is to quantify how minute-resolution affects capacity expansion results, system design decisions, and computational runtime. The study also evaluates the impact of lost load through unserved energy on system configuration and cost, highlighting how temporal resolution affects feasibility assessments and design outcomes. To manage the higher computational complexity associated with minute-resolution modeling, several complexity-reduction techniques like averaging, regular sampling, and clustering-based time series aggregation are assessed for their trade-offs between accuracy – total annualized cost and components sizing – and computational runtime. The results show that minute-resolution is essential for accurate photovoltaic-based single building systems, with this effect less pronounced in aggregated building systems. The inverter as a bottleneck between the demand and supply system is mostly affected in both the single and the aggregated building systems, and therefore should be systematically sized. On the complexity part, the results show that carefully selected aggregation approaches can preserve most of the accuracy of minute-resolution models while significantly reducing runtime. In particular, combinations of averaging with regular sampling and clustering-based time series aggregation methods can achieve near-minute-level accuracy with runtimes comparable to hourly models. The findings underline the balance between temporal resolution, computational complexity, and model accuracy. While minute-resolution offers better accuracy, appropriate aggregation methods can mitigate the computational burden. Future research could refine hourly data to enhance temporal detail while ensuring manageable computational complexity.

1. Introduction

The future energy systems are characterized by high shares of renewable energy to mitigate anthropogenic greenhouse gas emissions. However, renewable energy sources are inherently intermittent due to weather conditions and resource availability [1], making accurate modeling essential for reliable system design, expansion planning, and operation.

Energy system models (ESMs) are widely used to design, simulate, and optimize energy systems [2]. These models help energy planners and policymakers make economic decisions about energy systems [3–5]. A key modeling choice of renewable energy systems is the temporal resolution, which is the level of detail in the temporal representation of data and parameters within a model [6]. Most optimization-based ESMs rely on hourly data, which may sometimes prove sufficient for capturing seasonal and annual variations in long-term planning models [7,8]. However, model results may suffer in terms of accuracy and reliability when applied to off-grid renewable energy systems, where ensuring continuous system reliability under variable supply conditions is essential [9]. In such cases, sub-hourly temporal resolutions are often required to ensure accurate system design and reliable operation [10,11]. Because of this, and the continued acceleration of computing

* Corresponding author at: Forschungszentrum Jülich GmbH, Institute of Climate and Energy Systems, Jülich Systems Analysis (ICE-2), 52425 Jülich, Germany.
E-mail address: o.omoyele@fz-juelich.de (O. Omoyele).

https://doi.org/10.1016/j.ecmx.2026.102186
Received 29 September 2025; Received in revised form 29 July 2026; Accepted 30 July 2026
Available online 4 August 2026

power and optimization solvers, sub-hourly modeling of energy systems is gaining momentum [12,13].

Despite its advantages, sub-hourly modeling is hampered by limited data availability and exponential increase in computational runtimes [14]. Higher temporal resolution increases the number of variables and constraints, leading to larger and more complex optimization problems [15]. The drivers for model complexity in energy system optimization can span a range of factors, including but not limited to model formulation, system size, spatio-temporal representation, model robustness, scalability, and adaptability to diverse system configurations [16,17]. In terms of spatio-temporal complexity, stemming from the input data requirements, spatial resolution sometimes has a greater impact on model accuracy and reliability than temporal resolution, particularly in complex models. For instance, models with high spatial but low temporal resolution may remain feasible yet inadequately capture weather dynamics [18], while models with high temporal but low spatial resolution may oversimplify transmission constraints and system interactions [18,19].

While these complexity drivers are interrelated, this study focuses on temporal complexity arising from high-resolution time series data. The objective is to investigate the trade-off between model accuracy, reliability, and computational tractability, and how this trade-off differs between single-building and aggregated multi-building systems. Photovoltaic-based systems are analyzed at two scales: a self-sufficient building model, emblematic of conservative design principles, evaluated for two individual buildings with distinct demand profiles, and a microgrid model aggregating demands from six buildings (with a twelve-building configuration examined separately as a sensitivity case) to assess load aggregation effects. For each case, capacity expansion models are optimized using both minute- and hourly-resolution data. Total system cost and component sizing are compared to quantify inaccuracies introduced by hourly resolution at both scales, followed by a feasibility assessment through lost loads. To analyze the accuracy–complexity trade-offs, averaging, sampling, and clustering-based time series aggregation methods, using typical periods and segmentation, are applied to minute-resolution data.

Accordingly, this study addresses the following research questions:

- To what extent does the use of minute-resolution supply and demand data affect system cost, component sizing, and reliability outcomes, particularly under value of lost load (VoLL) analysis, when system designs are optimized at hourly resolution in islanded energy systems?
- How does increasing the number of demands influence the necessity of minute-resolution due to load aggregation and demand smoothing effects?
- How can temporal aggregation of minute-resolution time series improve the design and accuracy of energy system optimization results compared to hourly resolution, while maintaining comparable computational runtimes?
- Can a bootstrapping-based aggregation approach, using multiple parallel hourly representations derived from minute-resolution data, accurately approximate minute-resolution optimization results at significantly lower computational cost?

The remainder of this study is structured as follows: Section 2 conducts a comprehensive literature review on subhourly resolution modeling and the methods for mitigating temporal complexity. Subsequently, Section 3 presents the methodologies employed and the case studies investigated. Section 4 presents the results and discussions of the different case studies. Finally, Section 5 offers concluding remarks summarizing the major insights from the study.

2. Literature review

Several studies have investigated the impact of temporal resolution in energy system modeling, particularly the use of sub-hourly data [9,12]. A key finding is that sub-hourly resolutions down to one minute reveal significantly more detail than hourly resolution [20]. Minute-resolution improves the representation of short-term fluctuations in photovoltaic generation and demand, directly affecting system costs and component sizing [9]. Beyond cost and capacity outcomes, temporal resolution also influences reliability metrics such as lost load and unserved energy. Hourly resolution tends to smooth extrema present at minute resolution, minimizing the maxima and maximizing the minima, which can lead to underestimation of critical components capacities, especially in renewable-dominated and off-grid systems, consequently resulting in unserved energy [9,21]. Subhourly models are therefore better suited for capturing short peaks, rapid ramps, and inverter or storage bottlenecks that may trigger unmet demand. This has driven growing interest in high-resolution modeling for systems with stringent reliability and autonomy requirements. However, sub-hourly resolution substantially increases computational complexity compared to hourly modeling [9,22], making complexity reduction strategies essential.

The effectiveness of computational complexity reduction techniques depends on their ability to replicate the model solution of the fully operated time series [23], while reducing data dimensionality [24–26]. Averaging is the ubiquitous method for reducing the computational time of high-resolution time series in ESMs [9]. It involves calculating the mean or average of a set of values (see Fig. 1a and b), applied uniformly across the time series. Unlike segmentation (which is further discussed below), averaging does not adapt to gradients or variability in the data and therefore cannot retain higher resolution during periods of rapid change.

Sampling has also been used to reduce the computational complexity of energy systems by taking a regular sample of the input time series data (see Fig. 1b) [9]. Given the prevalence of hourly resolution in ESMs, hourly sampling has been widely adopted [22,27–30]. However, sampling generally leads to over- or under-estimation of the objective values [9]. Villoz et al. [30] represented a full one-minute resolution by calculating 60 different hourly resolutions, representing each minute by one hour and finding the average. Building on this work, Omoyele et al. [9] showed that sampling average methods does not accurately reproduce fully resolved minute-level behavior, although it perform better than simple hourly averaging.

Another widely used concept for reducing temporal complexity is the clustering-based time series aggregation, which describes the process of breaking down a continuous time series into distinct segments or intervals that exhibit recurring patterns or trends [15]. By aggregating similar periods, this approach reduces data dimensionality while preserving essential information [31]. The dimension reduction is achieved by using single longer time steps in place of a group of adjacent time steps (segments), or a cluster of days with similar diurnal profiles (typical days). The use of typical periods and resolution variation by segmentation are two major techniques for time series aggregation methods [24]. The typical period approach identifies recurrent temporal patterns and clusters time steps, most often days, into representative periods that collectively approximate the full time series (Fig. 1c) [32]. These periods may represent different seasons or weekdays based on demand and generation profiles. A representative period is then selected from each cluster to serve as a proxy [33]. Recent work has enhanced this approach through representative-hour methods and hybrid aggregations, improving the capture of short-term variability and storage dynamics while significantly reducing computational effort [34–36]. Segmentation aggregates adjacent time steps in a period that exhibits similar characteristics (see Fig. 1a) [24,32], reducing complexity while retaining temporal patterns [37]. Like typical periods, segmentation also uses clustering techniques to merge data and represent each cluster by a sample from the cluster or a synthesized representative that reflects the overall characteristics of the cluster. Recent advances allow variable segment lengths and explicitly incorporate operational constraints such as ramping and network limits, improving approximation accuracy in

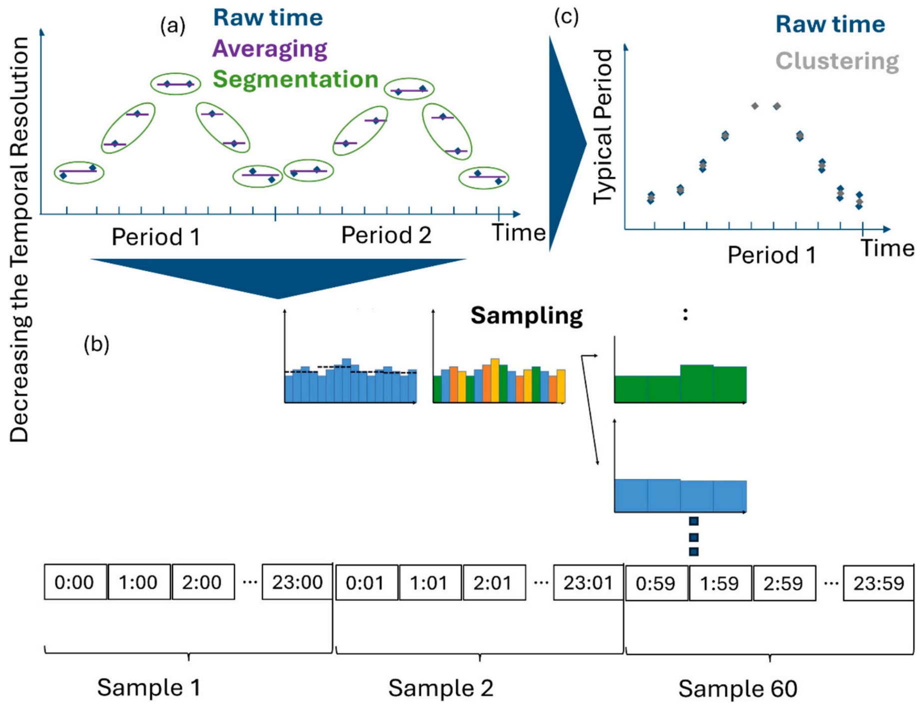

Fig. 1. Methods of temporal aggregation, adapted from Refs. [9,16]. (a) Raw time-series data are simplified through averaging and segmentation, reducing temporal resolution within each period. (b) Sampling-based aggregation selects representative time steps or profiles from the full series. (c) Clustering-based aggregation groups similar time steps into a limited number of typical periods.

power system optimization models [38].

K-means and hierarchical clustering are the two prevalent methods for aggregating consumption and renewable energy generation time series [39], alongside methods such as k-medoids, k-centres, k-shape, and k-MILP [24,40]. Kotzur et al. [40] found that while the choice of clustering algorithm has limited impact on optimal system design, Ward's hierarchical clustering offers reproducible results and a favorable trade-off between accuracy and computational tractability. Nevertheless, aggregation methods should be selected based on the specific characteristics and objectives of each modeling problem [24,32]. The importance of explicitly including extreme or rare periods has also been emphasized [41], with recent studies proposing systematic approaches for identifying and incorporating system-critical events [35].

Despite their advantages, time series aggregation methods are not exact and may lead to an under- or over-estimation of model results depending on the aggregation technique, data characteristics, and system configuration [9]. Nonetheless, recent studies demonstrate that carefully designed aggregation frameworks can achieve a robust trade-off between accuracy and computational efficiency [34,42], and in some cases yield exact or near-exact solutions even in the presence of intertemporal coupling, particularly for energy storage systems [36,38]. As such, time series aggregation remains a key enabler for solving large-scale-mixed-integer linear energy system models and exploring complex system designs that would otherwise be computationally intractable [43,44]. Against this background, this study investigates the impact of subhourly temporal resolution on both single-building and aggregated-building energy system designs using self-sufficient building and microgrid models. In addition to cost and capacity outcomes, the analysis explicitly evaluates lost load and unserved energy as reliability indicators. The study further compares multiple time series aggregation methods with respect to their ability to preserve minute-resolution cost and design capacity results while reducing computational complexity, as compared to hourly resolution.

3. Methodology

In the following, we present the impact of temporal resolution in energy system modeling and the different temporal aggregation techniques employed to reduce the computational complexity of energy systems, as well as the case studies.

3.1. Impact of temporal resolution in energy system modeling

To quantify the impact of temporal resolution on energy system design, reliability, and computational tractability, a structured modeling and optimization framework is applied across multiple temporal scales. The analysis compares minute-resolution models with hourly resolution ones while keeping all other model inputs, constraints, and techno-economic parameters constant. Deviations in cost, capacity sizing, and unserved energy are calculated in relative terms. This comparison allows identification of which components are most sensitive to temporal aggregation and whether aggregation effects differ between the single-building and microgrid cases, and to what extent. Particular attention is given to inverter sizing and storage operation, since these components are directly influenced by short-term variability and ramping behavior. Two photovoltaic-based case studies are considered: (i) a self-sufficient building representing a single-node off-grid system and (ii) a microgrid consisting of six aggregated buildings representing a multi-demand system (with a twelve-building configuration examined separately as a sensitivity case). These two cases enable the assessment of temporal resolution effects at both individual and aggregated load levels. The exposition of the self-sufficient building and microgrid models are shown in Sections 3.3.1 and 3.3.2, respectively. Minute-resolution time series are used as the reference dataset. These included electrical and thermal demands and photovoltaic generation profiles covering a full year. The minute-level dataset serves as the baseline against which hourly-resolution scenarios are evaluated. Reliability is modeled through an explicit unserved energy variable with a high penalty cost to ensure that lost load is only used when strictly necessary. This allows direct quantification of lost load and its sensitivity to temporal resolution.

To evaluate how temporal resolution affects system reliability, a two-step modeling procedure is applied. In the first step, the capacity expansion problem is solved using the full minute-resolution time series. The same model is then re-solved using the hourly resolution. This step quantifies the optimal component capacities and total annualized system cost. Hourly resolution is included as a benchmark since it represents the prevailing standard in many energy system optimization studies. In the second step, the impact of hourly temporal resolution on system reliability is assessed through a lost load analysis. The objective of this step is to test whether system designs obtained from hourly optimization remain operationally feasible when exposed to minute-level variability. For this purpose, capacities obtained from the hourly-resolution optimization are integrated in the optimization problems and a dispatch-only optimization is performed using the minute-resolution time series.

To guarantee solvability of the dispatch problem under peak capacities and assess whether the obtained system designs remain operationally feasible under high-resolution variability, which holds only when no auxiliary energy is required (i.e., unserved energy equals zero), an auxiliary electricity source is introduced whenever the system fails to meet the demand. This source represents a theoretical backup supply that provides electricity only when the designed system cannot satisfy demand under minute-level conditions. The energy supplied by this auxiliary source is interpreted as unserved energy (lost load) in the real system. In practical terms, it represents the amount of demand that would remain unmet if the system designed with hourly data were operated under true high-resolution variability. The auxiliary source is assigned a high variable cost based on the VoLL, which represents consumers' willingness to pay to avoid supply interruptions. The VoLL formulation therefore provides a reliability assessment by quantifying unserved energy, which also serves as an indicator of whether the optimized system design remains technically feasible under minute-resolution dispatch. Consequently, VoLL is used not only as an economic penalty parameter, but also as an indicator of technical infeasibility, as any non-zero unserved energy reveals that the optimized design cannot fully satisfy demand under high-resolution operation. This approach enables an explicit assessment of whether system designs derived from lower temporal resolution remain technically feasible under real high-frequency variability, rather than assuming feasibility a priori. Reported VoLL estimates for residential consumers typically fall in the range of €10–€25 per kWh, with survey-based values commonly around €10 per kWh [45,46]. In this study, a VoLL of €10/kWh is applied.

3.2. Methods for reducing the computational runtimes

For the clustering-based aggregation techniques, we use the Python package tsam,[1] which provides out-of-the-box aggregation techniques. The tsam is integrated into the ETHOS.FINE[2] [47,48] model framework used for optimizing arbitrary ESM instances [49,50], and open-source available on GitHub. It is continuously maintained and further developed by the authors of this manuscript within the ETHOS (Energy Transformation Pathway Optimization Suite) Model suite [51]. Since hourly resolution modeling is very ubiquitous in the literature, the averaging (just as used above) and sampling approaches will be used to derive time series at hourly resolution. Equation 1 represents the average hourly-resolution time series from minute-resolution ones.

$$X_{avg} = \left\{ x_i = \frac{1}{60} \sum_{k=1}^{60} x_{k,i} \, , \, i \in \{1, 8760\} \right\} \tag{1}$$

[1] https://github.com/FZJ-IEK3-VSA/tsam.
[2] https://github.com/FZJ-IEK3-VSA/FINE.

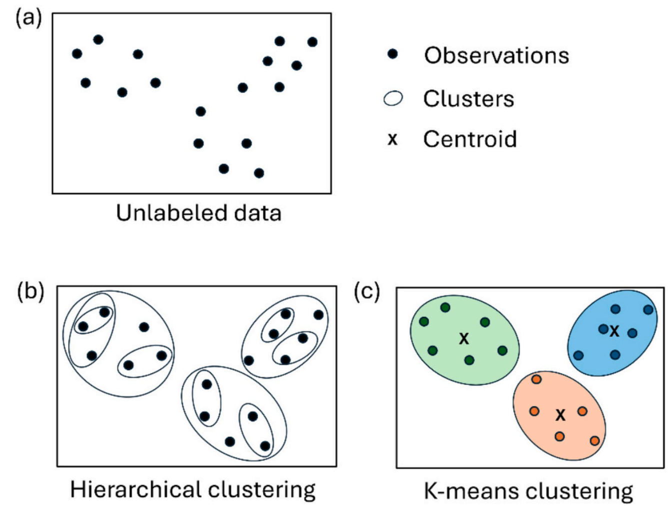

Fig. 2. Clustering techniques: (a) unlabeled data consisting of individual observations, (b) hierarchical clustering illustrating how observations are grouped into nested clusters based on similarity, and (c) K-means clustering showing partitioned clusters with their corresponding centroids (×).

Here, x_i represents the average value of the data points within the i th one-hour interval, and x_k represents the k th data point within hour i. Note that the time series used for optimizing the case studies has a length of one year.

The sampling is also taken at a one-hour resolution. Since there are 60 data points representing 60 min in each hour of the year, 60 different sets of hourly time series can be derived. Equation 2 shows the method for obtaining samples at every hour for the 60 different hourly time series.

$$X_{sam,k} = \{ x_{k,i} \, , \, i \in \{1, 8760\} \} \, \forall \, k \in \{1, 60\} \tag{2}$$

Here, we create k = 60 different hourly sample time series by forming one time series with 8760 time steps by taking the k^{th} minute-value from each hour of the original time series.

The clustering-based aggregation involves hierarchical clustering with typical periods and segments. The hierarchical clustering builds a multilevel hierarchy of clusters, which can be either agglomerative (bottom-up) or divisible (top-down) [52]. In divisive hierarchical clustering, the entire dataset starts as one cluster and is split recursively. By contrast, in agglomerative hierarchical clustering, each observation starts in its own cluster, and pairs are merged step-by-step, based on a selected linkage criterion. The algorithm is continued until all points are merged into one cluster (see Fig. 2b). The choice of linkage criterion significantly influences the clustering outcome. Common linkage methods include *single*, which considers the minimum distance between any two points in different clusters; *complete*, which uses the maximum distance between any two points in different clusters; *average*, based on

Table 1
Time series aggregation methods in "typical periods x segments", comparing fully resolved hourly data with representations based on typical days (24 segments) and typical weeks (168 segments).

Fully resolved hourly resolution	Typical days	Typical weeks
	1 × 24	
	5 × 24	1 × 168
	10 × 24	4 × 168
	20 × 24	8 × 168
	40 × 24	12 × 168
	80 × 24	24 × 168
	160 × 24	36 × 168
8760	365 × 24	52 × 168

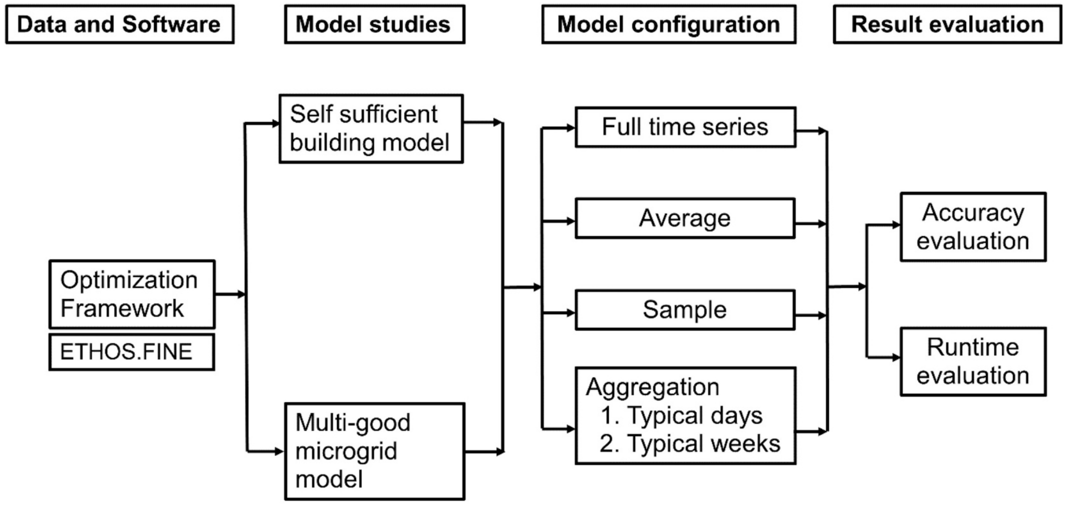

Fig. 3. Study setup, including the underlying modeling framework, model instances and configurations, and the evaluation methodology. The accurate solution considered is the result of the full time series dataset, while the accurate runtime considered is the computational runtime of the average one hour resolution time series.

the average distance between all pairs of points in two clusters; *centroids*, based on the distance between the cluster centroids; and *Ward's linkage* method (see Equation 3), which considers minimizing the increase in total within-cluster variance. Agglomerative clustering is considered in this study because of its efficiency.

$$\delta(C_i, C_j) = \frac{n_i n_j}{n_i + n_j} \|\mu_i - \mu_j\|^2 \tag{3}$$

where μ_i and μ_j are the centroids of cluster C_i and C_j for datasets x_i and x_j, respectively. n_i and n_j are the number of elements in the datasets x_i and x_j, respectively.

However, for sensitivity analyses, calculations are also made on k-means clustering. The K-means clustering is an unsupervised machine learning algorithm that partitions data points into a predefined number of clusters, denoted by k [53]. For instance, if $k = 3$, the algorithm will form three distinct clusters, as illustrated in Fig. 2c. The algorithm operates by iteratively determining the optimal positions of the k cluster centroids. Each iteration consists of two main steps: (i) Assignment: Each data point is assigned to the cluster whose centroid is closest, based on the Euclidean distance. (ii) Update: The centroids of the clusters are recalculated as the mean of the data points assigned to each cluster. These steps are repeated until the assignments stabilize (i.e., no significant changes occur) or a maximum number of iterations is reached, indicating convergence (see Equation 4).

Objective Function: Given a dataset $X = \{x_1, x_2, \dots x_n\} \subset R^d$, the objective is to find k clusters $C_1, C_2, \dots C_k$ that minimize:

$$\sum_{i=1}^{k} \sum_{x \in C_i} \|x - \mu_i\|^2 \tag{4}$$

where μ_i is the centroid of cluster C_i and $\|x - \mu_i\|^2$ is the square of the Euclidean distance between point x and the centroid μ_i.

To account for time-coupling beyond the length of a typical day or typical week, which is particularly relevant for modeling seasonal storage, our study relies on an approach described by Kotzur et al. [54]. For that, the entire year is represented by a sequence n of $\tilde{n}$ different typical days with $\tilde{n} \leq n = 365$ or a sequence m of $\tilde{m}$ different typical weeks with $\tilde{m} \leq m = 52$, i.e. each typical period can appear multiple times throughout the year. Along this sequence of typical periods, an additional set of constraints and variables is introduced at the interface between all typical periods and for each type of time-coupling variable from the original model formulation. This allows the transfer of state variables such as the state of charge of a storage from one period to another throughout the year, which not only enables the modeling of energy storage within typical days or weeks, but also the modeling of seasonal storage across these time spans.

Table 1 below shows the applied hierarchical-based clustering time series aggregation configurations, which are in typical days and typical weeks, denoted by the number of "typical periods x number of segments".

3.3. Case studies

To quantify our analyses, the ETHOS.FINE optimization framework is applied to two different models (see Fig. 3): a single-family self-sufficient building and a multi-good microgrid laboratory (MG2Lab[3]) with six different household time series representing six different buildings. For modeling the capacity expansion optimization of the self-sufficient building model, two distinct consumption demand datasets are considered using the building dataset described in Appendix A (Building 1 and Building 2). The building demand data are obtained using the SynPro[4] simulation tool, which produces high-resolution and valid synthetic performance profiles for residential buildings. The SynPro simulator combines physical models or measured load profiles with an occupancy behavior model driven by socio-economic parameters. It offers selectable profiles for electricity, heating, domestic hot water, and electric vehicles, tailored to some parameters such as building types, year of construction, building size and the number of occupants. The parameters are varied to generate different demand data for different buildings. Further information on SynPro is detailed by Fischer et al. [55,56]. The case studies apply a minute-resolution global horizontal irradiance measured by the Department of Energy at Politecnico di Milano [57].

With the two models, three different case studies are considered:

I. SSB1: Self-sufficient building for demand data 1 (Building 1 in Appendix A).
II. SSB2: Self-sufficient building for demand data 2 (Building 2 in Appendix A).
III. MG2Lab: Multi-good microgrid laboratory with combined data of six buildings.

[3] https://www.mg2lab.polimi.it.
[4] https://synpro-lastprofile.de/.

Each of the case studies is then optimized using the following model configurations:

I. Full-time series data in one minute.
II. Hourly averaged time series of the one-minute data.
III. Hourly samples of the one-minute data as shown in Fig. 1 and Equation 2.
IV. Advanced aggregation methods using typical days and typical weeks which are formed by the "number of typical periods x the number of segments" (Table 1).

Sections 3.3.1 and 3.3.2 present the self-sufficient building and the microgrid models considered, while the modeling resources used for the optimization is presented in Section 3.4.

3.3.1. The self-sufficient building model

Rising energy procurement costs and falling capital costs for renewable technologies could lead to a large number of off-grid buildings in the future [58]. As these fully self-sufficient systems cannot rely on imports from the grid if the system design is inadequate, the systems must be designed very accurately. In the present study, the self-sufficient building represents a residential island system which supplies energy through solar photovoltaic, inverter systems, conversion components (compressors, heaters and heat exchangers, and reversible fuel cell), and storage systems (battery, liquid organic hydrogen carriers, thermal storage, and hydrogen storage) as shown in Fig. 4. The self-sufficient building model was originally developed by Kotzur et al. [59], and further extended by Knosala et al. [60], Hoffmann et al. [26,61] and Refs. [44,62,63] for autonomous energy supply.

3.3.2. The multi-good microgrid laboratory model

For small communities and municipalities, the desire for self-sufficiency is also one of the most important incentives for investing in renewable energies [64,65]. However, in the past, these off-grid or microgrid systems were often only considered at an hourly time resolution of one year or even only a few representative weeks (e.g. Refs. [66,67]). Therefore, in this work, we also consider the impact of the temporal resolutions in a larger off-grid system using the microgrid of the MG2Lab. The MG2Lab, located in the Department of Energy, Politecnico di Milano, is a cutting-edge microgrid integrating different distributed energy resources (see Fig. 5). It works both in island mode and connected to the main electricity grid, and can feature multiple configurations (single/multi-node), including an AI implementation for optimal energy management [68]. The setup of the MG2Lab, as presented in Fig. 5, is also used for capacity expansion. As demand, we model the total electric and thermal demands of six different buildings (Appendix A) with the demand data generated from SynPro in a system without grid connection. The six demand time series are added to see the performance of our study on a composite building model. Detailed components definition, capacity, and connections of the MG2Lab are explained in Nespoli et al. [68].

3.4. Modeling resources

The two models are formulated as a mixed integer linear programming capacity expansion optimization problem with the objective of minimizing the total annualized cost (TAC) of the system as presented in Equation 5.

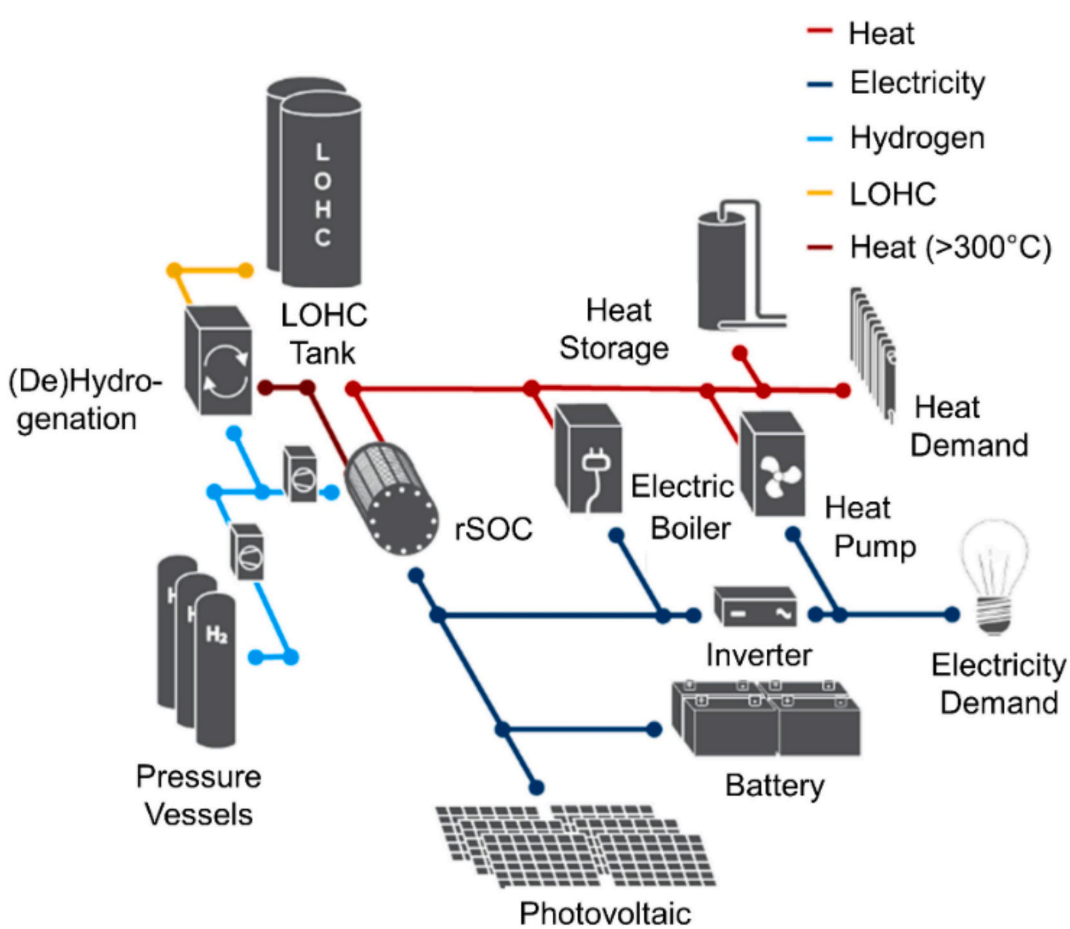

Fig. 4. Scheme of the self-sufficient building model as presented by Knosala et al. [60]. The rSOC is the reversible solid oxide cell and the LOHC is the liquid organic hydrogen carriers.

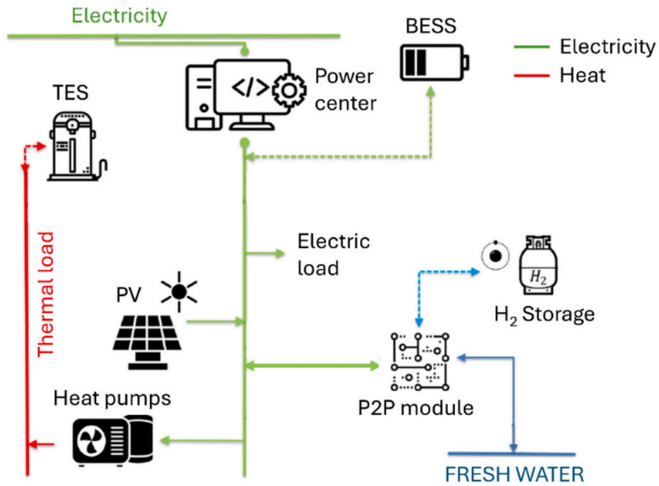

Fig. 5. Scheme of the MG2Lab model [68]. The BESS is battery energy storage systems, TES is thermal energy storage, P2P is power-to-power, PV is photovoltaic, and H_2 is hydrogen.

$$\mathrm{TAC} = \mathrm{CAPEX} \times \left(\frac{\mathrm{i}}{1-(1+\mathrm{i})^{-\mathrm{n}}} + \mathrm{OPEX}_{\mathrm{rel}}\right) \tag{5}$$

The TAC is the total annualized cost, CAPEX is the capital expenditure, $\mathrm{OPEX}_{\mathrm{rel}}$ is the operational expenditure relative to the capital expenditure, and i is the economic interest rate over the components' lifetime, n. The optimization problem is modeled using the ETHOS.FINE [47,48] optimization framework on a high-performance computing cluster using a fixed solver configuration. The techno-economic data and the complete optimization formulation used for all the case studies are shown in Appendices B and C, respectively. The computational resources are 8 CPUs-per-task, 1 compute node, 32000 MB mem-per-cpu, 32 threads, and 2 TB random access memory.

4. Results and discussion

Our results demonstrate that, compared to minute-resolution, using an average hourly resolution in the ESM leads to a substantial reduction in computational runtime by as much as 98% (see Table 2). However, there is an accuracy loss of only about 1% in TAC, particularly in the design of the self-sufficient building model (SSB 1 and SSB 2). This suggests that using hourly resolution may not be critical for capturing total system costs. Nevertheless, while the impact of minute-resolution input data on system costs is relatively small, such high temporal resolution may still be essential for ensuring system feasibility and reliability—especially in off-grid contexts. As discussed by Omoyele et al. [9], underestimated capacities of dynamic components (e.g., storage and inverter) due to insufficient temporal granularity can lead to system infeasibility in off-grid energy systems. The reliability assessment, based on the quantification of unserved energy in the system, shows that hourly resolution is insufficient to capture the variability present in the minute-resolution time series, resulting in technically infeasible system designs for the self-sufficient building under minute-resolution operation. Specifically, the dispatch analysis identifies lost loads of 31 kWh for SSB1 and 25.4 kWh for SSB2 (Fig. 6 and Fig. 7). These values represent the amount of unmet electrical and thermal demands, while the corresponding VoLL penalty (€10/kWh) quantifies their economic impact. Therefore, considering the VoLL would make the increase in costs much more significant. The increased runtime and the problem of limited data availability at minute-resolution may lead many modelers and scientists to continue modeling energy systems with average hourly resolution data in the future. Instead, a high safety factor may be utilized for heavily undersized capacities.

The accuracy loss between the hourly and minute-resolutions for the larger system of the MG2Lab, comprising combined time series data (six buildings), is only 0.37% (see Table 2, Table 7, and Appendix D). This likely stems from the aggregation effects inherent in larger, more diverse systems. In this case, temporal fluctuations tend to average out, reducing the impact of high-frequency variability on system design and operation. This smoothing effect dampens the influence of sub-hourly resolution compared to a single-building model, where demand and supply dynamics are more tightly coupled and subject to sharper intra-day variations.

While the aggregated-building analysis provides insight into the influence of temporal resolution on systems with increasing scale, further investigations are conducted for systems comprising between one and twelve aggregated buildings supplied by a single, shared off-grid energy system (see Fig. 8). For these analyses, the demand data for multiple buildings are aggregated additively, and the systems are modeled in an off-grid configuration. The results, Fig. 8, demonstrate that high-resolution data lead to larger deviations in both cost and component capacities compared with hourly resolution. However, as the number of aggregated buildings increases, the effect of temporal resolution on cost and inverter capacity diminishes due to the smoothing effect inherent in aggregated demand profiles. This effect occurs because the peaks of individual building load profiles often coincide with the troughs of others, thereby reducing overall variability. As shown in Fig. 8a, the TAC stabilizes beyond four aggregated buildings, where the underestimation decreases from 0.9% to 0.4%, with minimal changes thereafter. The inverter capacity exhibits the highest sensitivity to temporal resolution, with deviations reaching up to 50%, as also in the cases of SSB 1 and SSB 2 (see Fig. 8b), particularly in smaller systems. As the number of buildings increases, this deviation gradually reduces and stabilizes at

Table 2
Results of the minute and hourly resolutions for the considered cases in terms of the total annualized cost and the associated computational runtime (in brackets).

	SSB 1	SSB 2	MG2Lab
Fully resolved in one minute	3623.09 € (254273.71 sec)	3362.94 € (129052.97 sec)	22545.06 € (25811.59 sec)
Averaged one hour resolution	3589.36 € (3991.02 sec)	3340.05 € (2337.97 sec)	22461.65 € (28.56 sec)

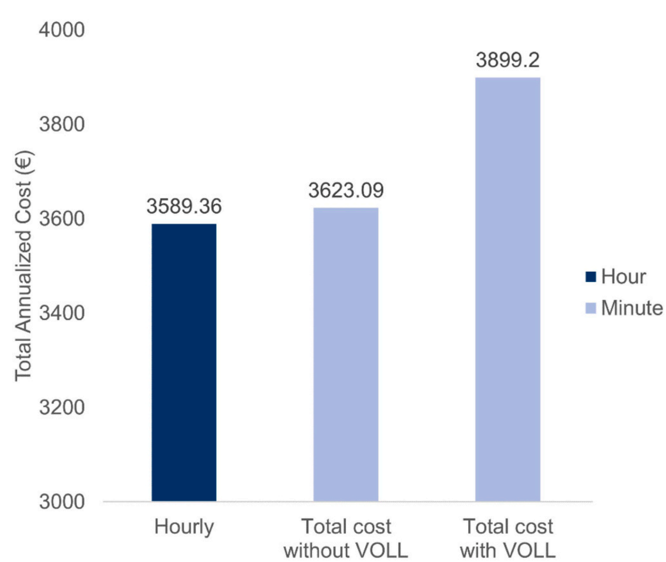

Fig. 6. Total annualized cost in SSB 1 for hourly- and minute-level resolutions, with and without the value of lost load (VoLL). The system design is optimized at hourly resolution and evaluated using minute-resolution data.

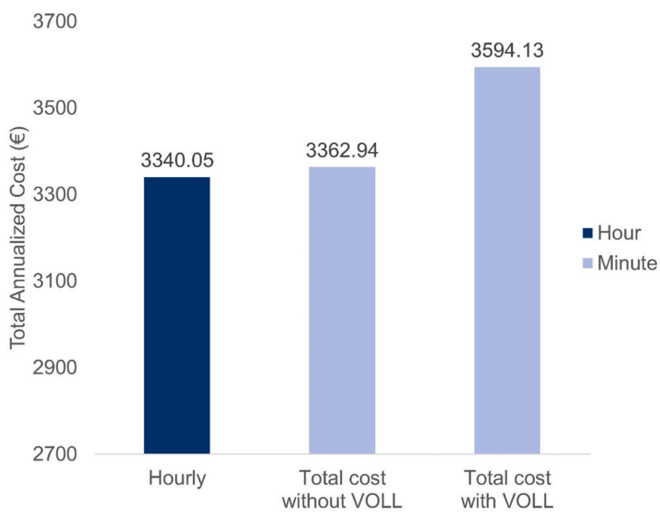

Fig. 7. Total annualized cost in SSB 2 for hourly- and minute-level resolutions, with and without the value of lost load (VoLL). The system design is optimized at hourly resolution and evaluated using minute-resolution data.

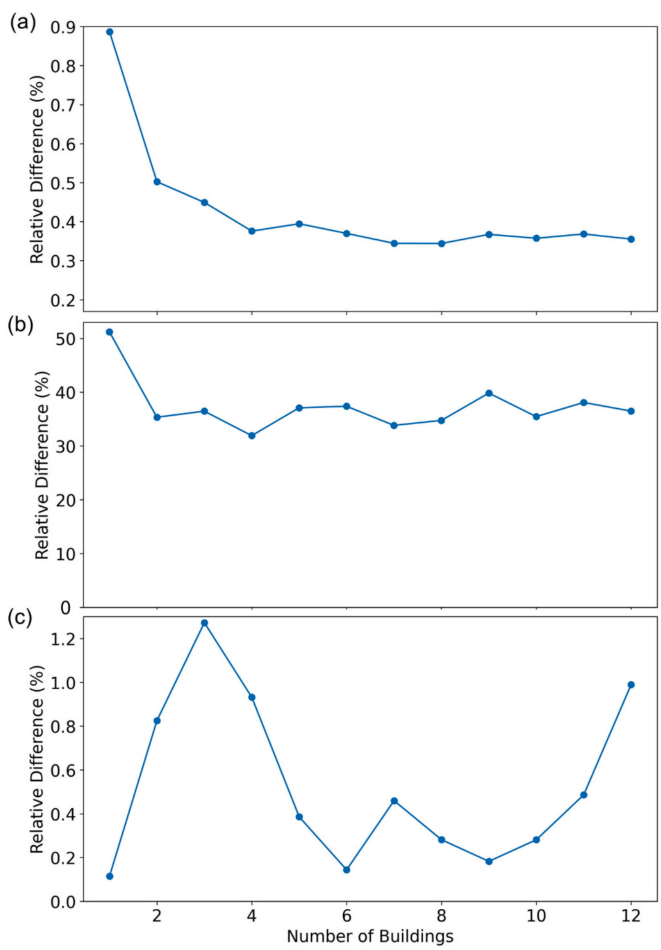

Fig. 8. Relative difference between hourly- and minute-resolutions on the number of buildings for (a) total annualized cost, (b) inverter capacity, and (c) battery capacity. The relative difference is the percentage deviation of the hourly-resolution result from the corresponding minute-resolution result.

approximately 35% for the minute-based resolution. In contrast, the battery capacity demonstrates a highly variable or spiky behavior (see Fig. 8c). The underestimation in battery capacity is relatively small compared with the inverter capacity, but its instability reflects the battery's role in buffering the residual variability within the system. These findings highlight the pronounced impact of fine temporal resolution on small-scale, self-sufficient systems such as single buildings, where hourly resolution can significantly underestimate both system cost and component capacity. In larger systems, such as multi-family buildings or district-scale configurations, the smoothing effect of aggregated demand profiles reduces variability and mitigates underestimation errors, thereby improving the design inaccuracies of lower-resolution modeling approaches.

Therefore, in composite or larger-scale systems, hourly resolution may be sufficiently representative for capturing key system behaviors, while in smaller or more isolated systems (such as off-grid buildings), the omission of sub-hourly variability can lead to greater design inaccuracies [7,8]. This insight suggests that the optimal temporal resolution may scale with system size and heterogeneity, a relationship that warrants further investigation.

The sampling results comprise 60 different samples, as shown in Fig. 1, and then 60 different optimal solutions representing the 60 min in between hourly resolutions shown in Fig. 9 for the three case studies considered. Fig. 9 shows the results of the TAC for the 60 different samples, benchmarked by the fully resolved result in one-minute resolution and the hourly-averaged resolution result, as well as the average result over all sampling results. The full results comprising the TAC and the installed capacities of the highly dynamic systems are presented in Figs. 17–19 of Appendix E. The results demonstrate that some samples can produce almost fully accurate results. However, since such samples cannot be deciphered before the optimization, the average of the results of all the samples is taken. The sampling average produces a much better result in terms of the TAC (Fig. 9) and components' sizing (Figs. 17–19 of the Appendix E) as compared to the common method of averaging the time series data. Overestimations of 0.076%, 0.12%, and 0.12% are observed for the TAC of SSB1, SSB2, and MG2Lab, respectively, at an approximate computational runtime of one hour resolution models due to cluster parallel arrays for the 60 different hourly resolution models.

The clustering-based aggregation techniques with varying typical periods and segments are a more advanced method for reducing the computational runtime of an ESM. The results obtained from the capacity expansion optimization of the case studies with time series aggregation are presented in Table 3 and Figs. 10–15. Table 3 shows different typical days and weeks (as presented in Table 1) and the TAC results with the associated computational time of the optimization problem. Figs. 10–12 show the comparison of the different aggregation periods and segments considered for the accuracy and runtime for SSB 1, SSB 2, and the MG2Lab, respectively. The accuracy is the optimal solution of the TAC from the fully resolved one-minute resolution (which is the target accurate solution), and the runtime is the computational time of the optimal solution of the average hourly resolution (which is the target computational runtime), which are presented in Table 3. Figs. 13–15 represent the capacity deviation (in percentage) from the minute-resolution optimizations for the time series aggregation methods considered in Table 1, using typical days and typical weeks, respectively. The TD1 (1 typical day, represented by 1x24) and TW1 (1 typical week, represented by 1x168) are not considered in Figs. 10–15 because they show too high deviations, however, they are presented in Table 3.

While large aggregation reduces the computational time at the cost of huge inaccuracies in the result, less aggregation gives a good accuracy at the cost of longer computational runtime. 24 segments per typical day show very good results in terms of both the TAC (Table 3 and Figs. 10–12) and the installed capacities (Figs. 13–15) of the components for more than 160 typical periods. 365 typical periods x 24 segments show 99.78% accuracy and an improvement of 76.6% of the underestimated average hourly TAC for SSB 1. Also, 365 typical periods x 24 segments show 99.97% accuracy and an improvement of 96.8% of the underestimated average hourly TAC for the SSB 2. With MG2Lab showing good accuracy at hourly resolution, the hierarchical clustering

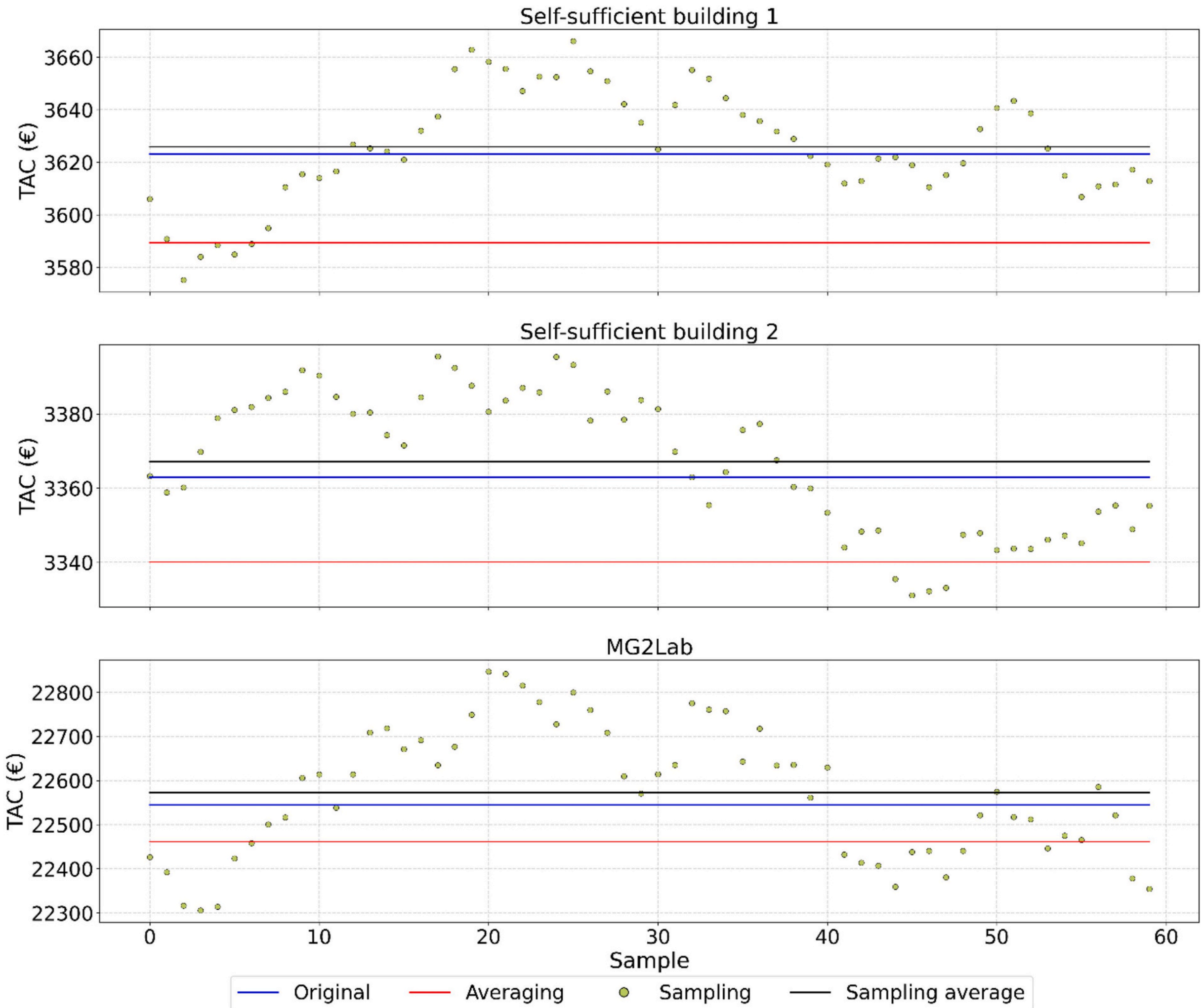

Fig. 9. Total annual cost (TAC) for the original or fully resolved minute data (original), averaging of the data, sampled data (sampling), and the average of the sampled result, for the case studies.

Table 3
Results of the aggregation methods for the considered cases in terms of the total annualized cost and the associated computational runtime (in brackets). Aggregations are applied to the minute-resolution data.

Typical days				Typical weeks			
	SSB 1 (Time, secs)	SSB 2 (Time, secs)	MG2Lab (Time, secs)		SSB 1 (Time, secs)	SSB 2 (Time, secs)	MG2Lab (Time, secs)
1 × 24	1271.70 € (1.86 sec)	1210.00 € (1.80 sec)	4909.90 € (0.81 sec)	**1 × 168**	1290.28 € (38.36 sec)	1218.98 € (7.64 sec)	4939.01 € (1.06 sec)
5 × 24	3556.03 € (15.73 sec)	3295.57 € (9.50 sec)	21501.86 € (0.78 sec)	**4 × 168**	3612.95 € (26.50 sec)	3314.83 € (26.76 sec)	21543.83 € (1.68 sec)
10 × 24	3675.63 € (9.85 sec)	3359.57 € (13.83 sec)	19649.67 € (1.19 sec)	**8 × 168**	3708.49 € (158.35 sec)	3385.06 € (118.84 sec)	20650.04 € (1.76 sec)
20 × 24	3704.37 € (87.70 sec)	3356.19 € (27.75 sec)	23864.89 € (1.85 sec)	**12 × 168**	3643.64 € (170.39 sec)	3347.99 € (306.45 sec)	19526.92 € (2.97 sec)
40 × 24	3695.44 € (70.09 sec)	3386.06 € (188.67 sec)	24037.48 € (3.43 sec)	**24 × 168**	3681.08 € (2087.54 sec)	3419.44 € (1785.14 sec)	24474.63 € (15.04 sec)
80 × 24	3670.17 € (194.82 sec)	3373.93 € (354.63 sec)	23840.65 € (5.73 sec)	**36 × 168**	3719.11 € (3385.27 sec)	3395.68 € (5022.67 sec)	24166.91 € (27.22 sec)
160 × 24	3649.47 € (671.37 sec)	3381.92 € (464.46 sec)	23061.46 € (9.54 sec)	**52 × 168**	3695.27 € (27310.89 sec)	3375.68 € (7642.16 sec)	24077.97 € (63.56 sec)
365 × 24	**3615.20 € (1153.72 sec)**	**3362.22 € (1089.99 sec)**	**22525.71 € (31.79 sec)**				

method still gives a 99.91% accuracy and a 76.8% improvement of the underestimated average hourly TAC. The components' size deviations are presented in Figs. 13–15, with 365 typical periods x 24 segments (TD 365) showing the least deviations (between −10.4% and 3.0%) from the original capacity obtained from one minute resolution in percentage. When the MG2Lab system is connected to the main electricity grid—allowing for electricity imports at a rate of 0.4 €/kWh—the TAC underestimation observed under hourly resolution becomes even less

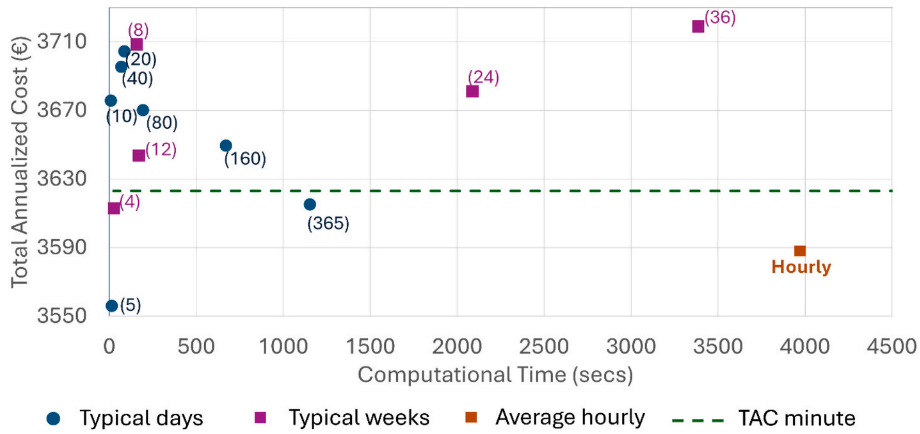

Fig. 10. Comparison of the time series aggregation in typical days (in blue) and typical weeks (in purple) to total annualized cost (TAC) of the fully resolved data and the computational time of the average hourly data for SSB 1. 10 typical days means 10x24 and 8 typical weeks means 8x168.

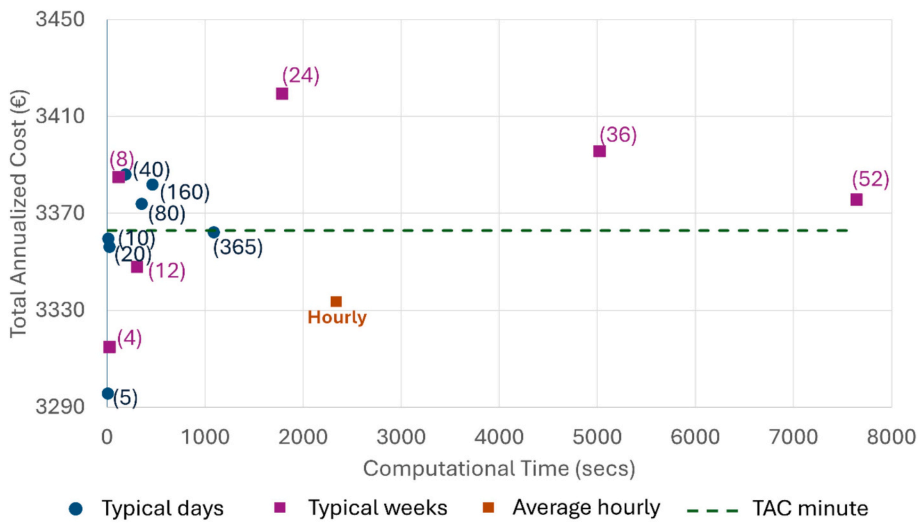

Fig. 11. Comparison of the time series aggregation in typical days (in blue) and typical weeks (in purple) to total annualized cost (TAC) of the fully resolved data and the computational time of the average hourly data for SSB 2. 10 typical days means 10x24 and 8 typical weeks means 8x168.

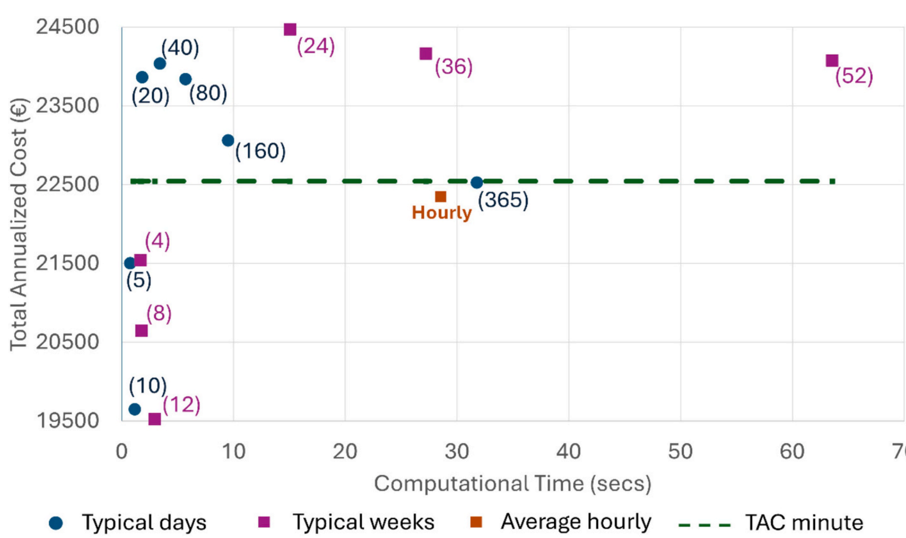

Fig. 12. Comparison of the time series aggregation in typical days (in blue) and typical weeks (in purple) to total annualized cost (TAC) of the fully resolved data and the computational time of the average hourly data for MG2Lab. 10 typical days means 10x24 and 8 typical weeks means 8x168.

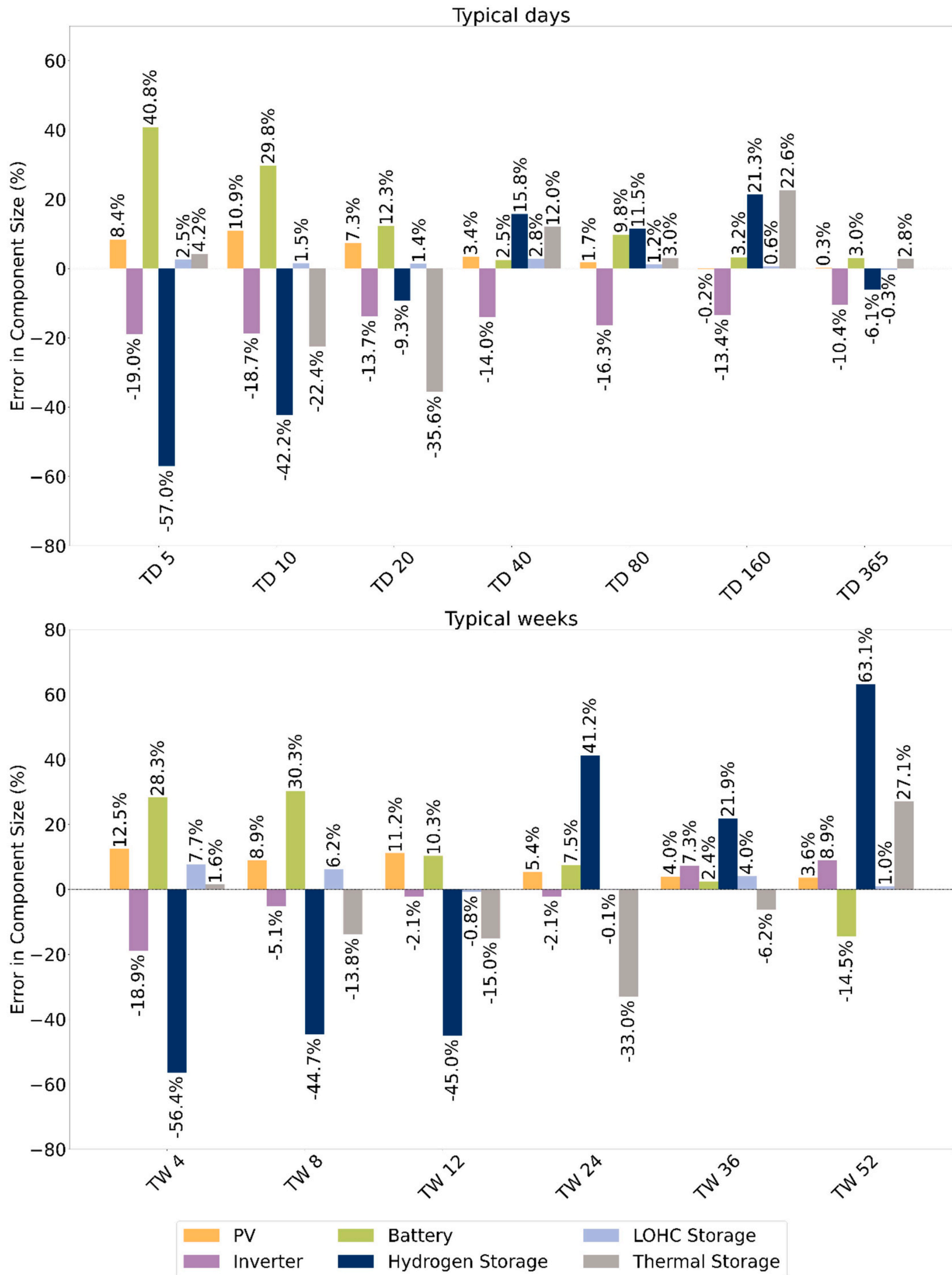

Fig. 13. Components capacity deviation from the fully resolved capacity using typical days (TD) and typical weeks (TW) in percent for the SSB 1.

significant (Appendix D). For the configuration, the deviation is reduced to 0.26%. In this grid-connected system, the 365 typical periods x 24 segments still show an accuracy of 99.98% and a 94.7% improvement of the hourly underestimated TAC. More results about the sensitivity of the MG2Lab microgrid with the buildings modeled as off-grid and grid-connected can be found in Table 5 and Table 6 of Appendix D. This finding reinforces the earlier conclusion that hourly resolution is generally sufficient for larger, grid-connected, or composite energy systems. In contrast, sub-hourly resolution remains critical for accurately modeling smaller-scale or off-grid systems, where system dynamics are more sensitive to high-frequency variability.

While the combined time series data of the buildings may have small variability, the average hourly resolution of MG2Lab may produce a good result as compared to some of the other aggregation methods considered. However, combined time series data do not always even out in variability, as the variability change depends largely on the

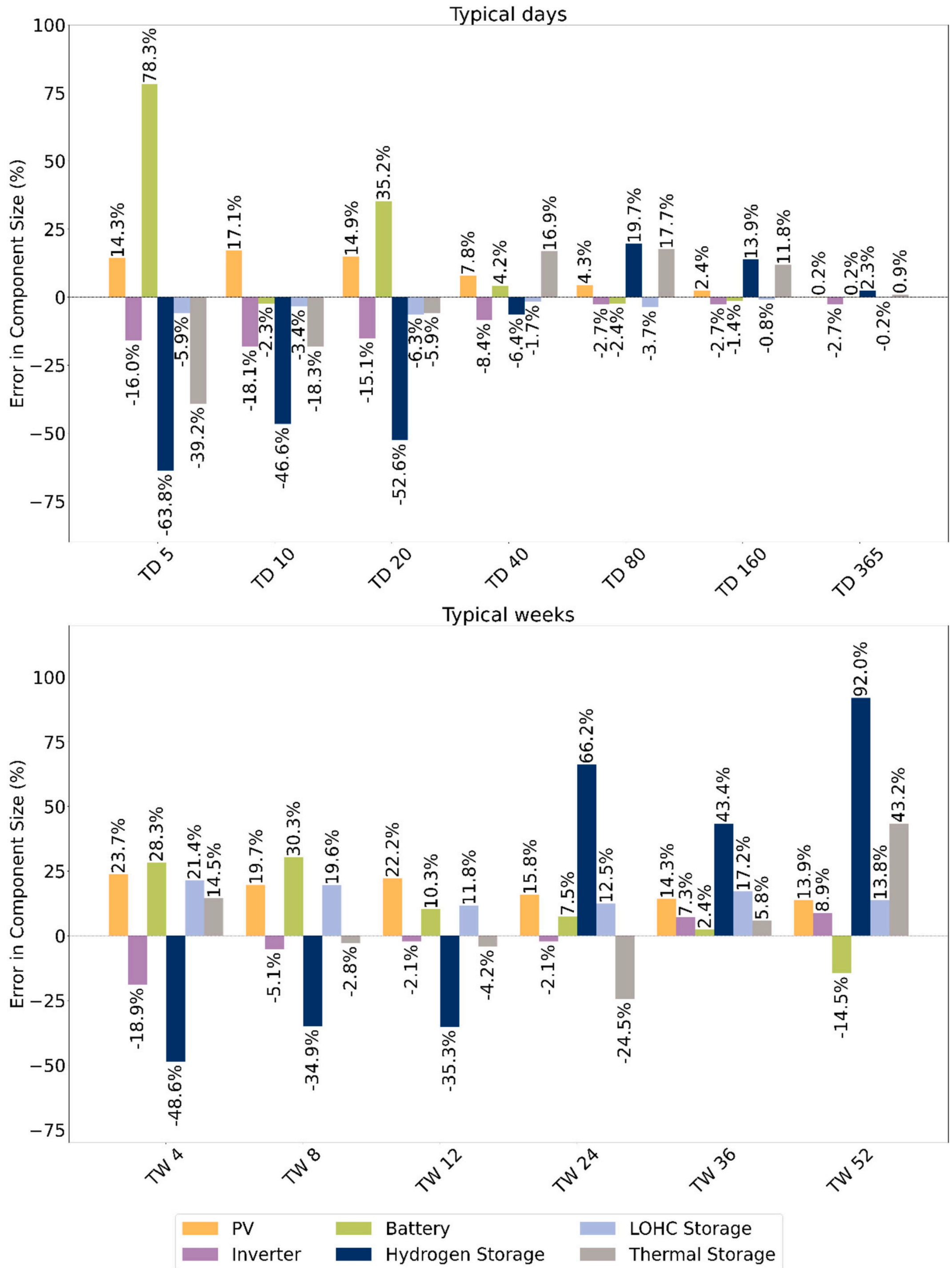

Fig. 14. Components capacity deviation from the fully resolved capacity using typical days (TD) and typical weeks (TW) in percent for the SSB 2.

distribution of each of the time series data. Even though hourly resolution gives a good performance for MG2Lab, the 365 typical periods x 24 segments aggregation method may still be applied to composite models because it deals appropriately with different data distributions and the accuracy is appropriately managed. 365 typical periods x 24 segments also show a very good computational runtime for all the cases considered, equivalent to the runtime at hourly resolution. The application of typical weeks does not show as good results as in the case of typical days, in terms of accuracy, computational runtime, and component sizing (Table 3, Figs. 10–12, and Figs. 13–15). Sensitivity analysis on SSB1 shows (i) the clustering methods considered (hierarchical, k-means, and k-medoids) do not affect the optimal solution of the system, Table 8 (ii) the robustness of the analysis by considering systems with different uncertainty configurations between 5 and 10% deviations

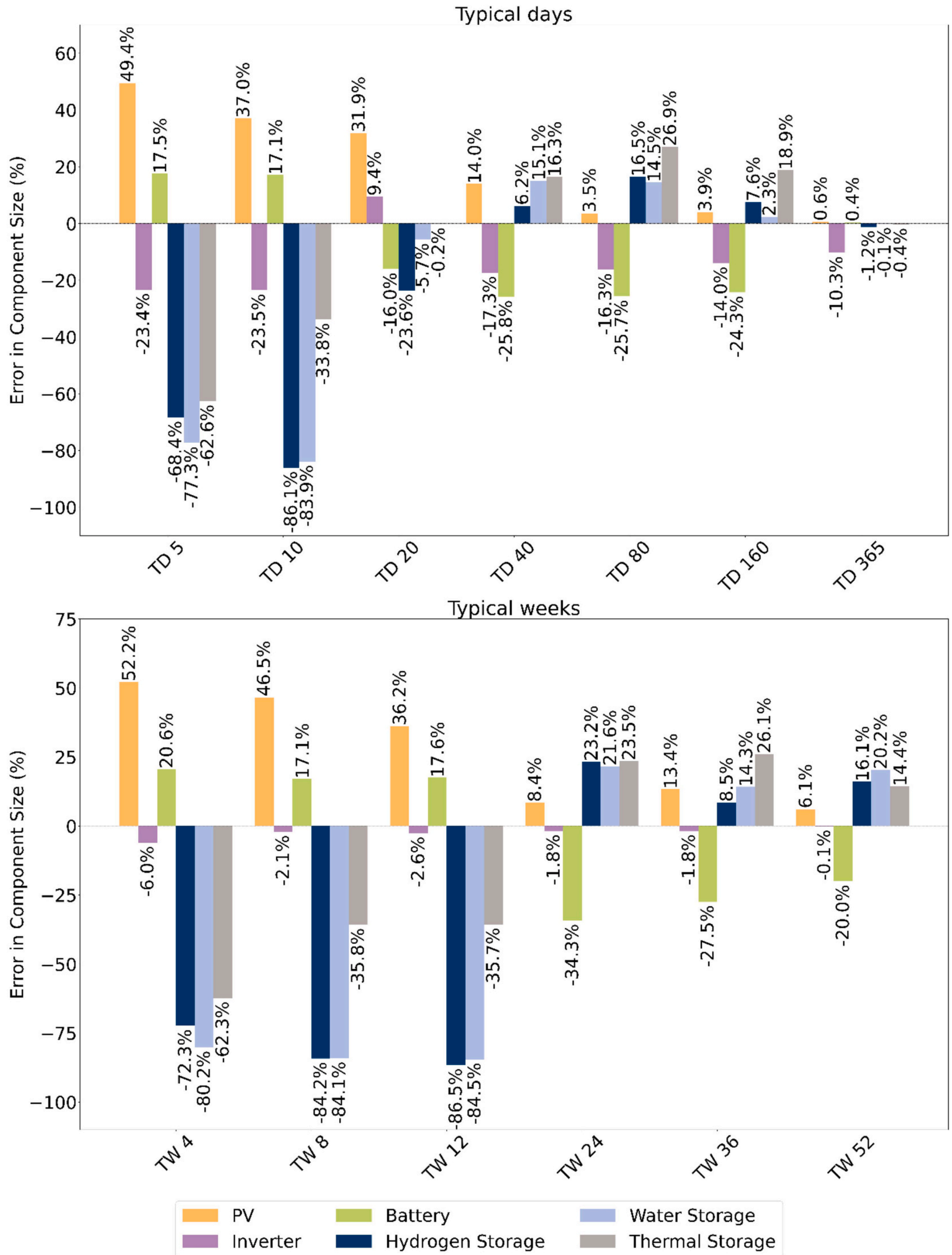

Fig. 15. Components capacity deviation from the fully resolved capacity using typical days (TD) and typical weeks (TW) in percent for the MG2Lab.

in both supply and demand data, Table 9. The results produce a similar result to the original model (SSB1), both in terms of hourly cost underestimation and the cost recovery by the clustering-based time series aggregation.

In a further sensitivity analysis, the full operated hourly time series resolution (8760) is further investigated using different typical periods x segments variations between typical days of maximally 365 × 24 time steps and typical weeks of maximally 52 × 168 time steps (in which the product of typical periods and segments is close to 8760 data points). The results presented in Table 4 and Fig. 16 indicate that the 365 × 24 configuration yields the most effective balance between TAC accuracy and computational efficiency for the considered cases. This configuration leverages 365 typical periods to preserve the full extent of inter-day and seasonal variability, while each day is discretized into 24 representative segments, effectively capturing the essential intra-day dynamics of energy demand and supply. Such temporal structuring aligns

Table 4
Sensitivity analysis of the total annualized cost results of the clustering-based aggregation methods for the three considered cases.

Aggregation	SSB 1 (€)	SSB 2 (€)	MG2Lab (€)
365 × 24	3615.20	3362.22	22525.71
244 × 36	3636.51	3372.34	22825.27
182 × 48	3645.89	3380.60	22937.09
146 × 60	3664.79	3385.67	23069.48
122 × 72	3663.42	3394.39	23318.09
105 × 84	3670.31	3397.49	23476.94
91 × 96	3674.94	3394.02	23741.91
81 × 108	3676.88	3374.18	23855.31
73 × 120	3685.04	3351.50	23842.23
63 × 132	3697.00	3361.44	23863.24
61 × 144	3682.61	3362.75	23855.76
56 × 156	3691.38	3365.52	24011.17
52 × 168	3695.29	3375.68	24077.96
Original	3623.09	3362.94	22545.06

naturally with the diurnal characteristics of solar photovoltaic generation, which exhibits predictable daily patterns modulated by seasonal shifts. By applying hierarchical clustering to reduce the original one-minute resolution data to 24 segments per day, the approach retains the most statistically and operationally relevant time steps—particularly around sunrise, midday peak, and sunset—thereby preserving system-critical events without the computational burden of the full-resolution dataset. As a result, the 365 × 24 formulation on the minute-resolution data achieves near-equivalent accuracy to the full-resolution model (within 0.1% TAC deviation) while maintaining computational runtimes comparable to conventional hourly simulations. Given this strong alignment with the underlying physical and operational characteristics of photovoltaic-based renewable energy systems, the average of the regular samples and the clustering-based aggregation of 365 typical periods with 24 segments are recommended as computationally tractable and accurately representative solutions for high-resolution energy system optimization models.

This study primarily focuses on the computational evaluation of temporal resolution methods in energy system modeling, using high-resolution simulations to quantify trade-offs between model accuracy and computational runtime. While the methods can be integrated into modeling platforms, their primary value lies in improving energy systems design. By capturing key dynamics with lower computational runtime, the system enables more accurate system cost and component sizing, thereby reducing the risk of power outages and lost loads, particularly in off-grid or self-sufficient systems. The lost load feasibility test described in Section 3.1 is applied only to the hourly-resolution benchmark design; the feasibility of the recommended aggregated designs (e.g., 365 typical periods x 24 segments) under full minute-resolution operation is not separately validated, and the reliability claims made for these aggregated approaches should be read as accuracy relative to the minute-resolution design rather than as an independent guarantee of operational feasibility.

Despite these contributions, several limitations remain. The analysis is limited to solar photovoltaic as a renewable energy source, which exhibits regular diurnal patterns. As a result of this, further studies should be conducted on wind power with less variability and a less regular supply pattern compared to solar irradiance. In addition, other self-sufficient systems with novel storage types could be investigated [50,69]. Additionally, the study partly relies on simulated input data, without accounting for uncertainties such as measurement noise or data quality. These uncertainties could influence the performance and accuracy of temporal aggregation methods and may be considered in future research. Furthermore, future studies using multi-year weather data would be beneficial to better assess system robustness and long-term reliability under varying climatic conditions [70]. Finally, yet importantly, the study has revealed at times counter-intuitive jumps in runtime from one model configuration to another, indicating that tuning

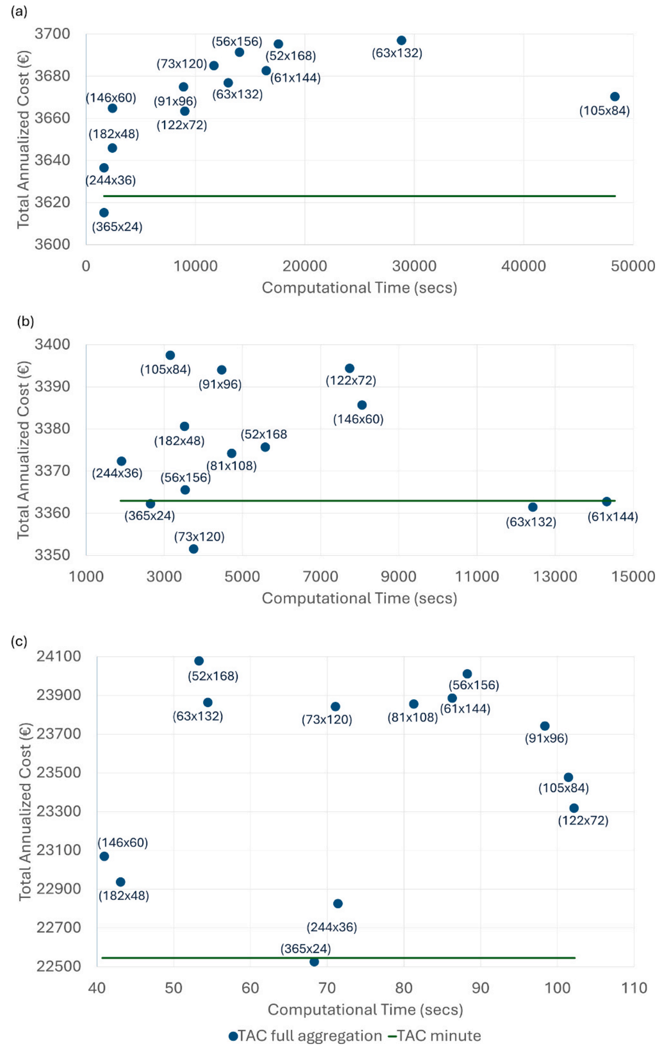

Fig. 16. Comparison of the full one-hour time series aggregation in typical periods x segments to total annualized cost (TAC) of the fully resolved data and the computational time of the average hourly data for: (a) SSB 1, (b) SSB 2, and (c) MG2Lab.

of numerics using out-of-the-box solvers such as Gurobi is still inevitable.

5. Conclusions

Sub-hourly resolution in energy system optimization improves the representation of short-term variability and component bottlenecks compared to hourly modeling, but significantly increases computational cost, motivating the use of temporal complexity reduction methods such as averaging, sampling, and clustering-based time series aggregation. This study reveals the following:

- The need for minute-resolution is highest for island systems with a value of lost load analysis when applying minute-resolution supply and demand time series to a system designed using hourly time series. This need decreases for larger numbers of individual and low-correlated demand profiles, such as in neighborhoods with multiple households supplied by a single system due to load balancing and a smoother resulting total demand profile.
- Aggregated time series provide a closer approximation to the minute-resolution total annualized cost and component sizing

than hourly time series, while maintaining runtimes comparable to hourly models.
- A bootstrapping method that generates 60 hourly profiles out of a minute-resolution time series, solves them in parallel and forms the average, creates a close approximation of the solution obtained for minute-resolution model, at an equivalent runtime of hourly resolution model.

The findings indicate that studies based solely on hourly resolution may underestimate required investments and overestimate system adequacy in decentralized and renewable-dominated settings, with implications for building energy codes, microgrid design guidelines, and resilience planning frameworks. In contrast, the need for sub-hourly profiles is less pronounced in highly interconnected systems, such as high-level national studies, where spatial balancing across large regions can mitigate short-term variability, and hourly resolution may be sufficient for high-level studies. However, for narrow system scopes such as self-sufficient buildings, microgrids, and off-grid systems, higher safety margins are required, and policymakers and regulators should therefore consider temporal resolution requirements, sub-hourly validation, or approved aggregation procedures when using optimization results to support decisions on self-sufficient buildings and local energy systems.

Ethical declaration

The author(s) declare(s) that the study does not involve humans nor animal subjects.

CRediT authorship contribution statement

Olalekan Omoyele: Writing – review & editing, Writing – original draft, Visualization, Validation, Software, Resources, Methodology, Investigation, Formal analysis, Data curation, Conceptualization. **Maximilian Hoffmann:** Writing – review & editing, Supervision, Formal analysis, Conceptualization. **Jann Michael Weinand:** Writing – review & editing, Visualization, Validation, Formal analysis, Conceptualization. **Detlef Stolten:** Supervision, Funding acquisition.

Declaration of Generative AI and AI-assisted technologies in the writing process

During the preparation of this work the author used the tools "ChatGPT and DeepL" in order to improve the readability and style in a few sentences. After using this tool, the author reviewed and edited the content as needed, and takes full responsibility for the content of the publication.

Declaration of competing interest

The authors declare that they have no known competing financial interests or personal relationships that could have appeared to influence the work reported in this paper.

Acknowledgements

This work was supported by the Helmholtz Association under the program "Energy System Design".

Appendix

A. Building demand data parameters from SynPro simulator for Berlin, 2021

		Building1	Building2	Building3	Building4	Building5	Building6
Number of occupants		4	3	4	4	4	3
H_ceiling/ww_ratio		2.4/0.2	2.4/0.2	2.5/0.25	2.4/0.2	2.4/0.2	2.37/0.3
Size (m^2)		200	150	200	180	220	205
Height (Stories)		1	1	2	2	2	1
Annual demand (kWh)	Electricity	3087.85	2827.54	3050.98	1913.98	1947.52	3001.90
	Heat	16257.05	14816.44	16611.26	15323.71	14343.71	16436.09
Mean (kWmin)	Electricity	0.3525	0.3228	0.3483	0.2185	0.2223	0.3427
	Heat	1.8558	1.6914	1.8963	1.7493	1.6374	1.8763
Standard deviation (kWmin)	Electricity	0.5109	0.5032	0.4930	0.3508	0.3648	0.5084
	Heat	1.9761	1.7955	2.0088	1.8804	1.6945	1.9902

B. Cost parameters of the self-sufficient building model according to Knosala et al. [60]

	Capex			Opex	Lifetime (years)	Components	Efficiency	
Components	Fixed (€)	Capacity-specific		Fixed + capacity-specific (% inv/a)				
Photovoltaic ground	—	4000.00	€/kW_p	1.00	20	Inverter		97%
Photovoltaic rooftop	—	769.00	€/kW_p	1.00	20	Lithium-ion battery	$\eta_{ch.\ and\ dis.}$	95%
Inverter	—	75.00	€/kW_p	—	20		Self-discharge	0.01%/h
Battery	—	301.00	€/kWh_p	—	15	Redox flow battery	$\eta_{ch.\ and\ dis.}$	86.6%
Reversible Solid Oxide Cell	5000.00	2400.00	€/kW_{el}	1.00	15	PEM fuel cell	η_{el}	55%
Heat pump	4230.00	504.90	€/kW_{th}	1.50	20	PEM electrolysis	η_{el}	70%
Thermal storage	—	90.00	€/kWh_{th}	0.01	25	rSOC electrolysis mode (w/o heat integration)	ηH_2	73.2%
E-Heater & e-boiler	—	60.00	€/kW_{th}	2.00	30	rSOC fuel cell mode	ηH_2	45%
Tank	—	0.79	€/kWh_{H2}	—	25		η_{el}	35%
Dibenzyltoluene	—	1.25	€/kWh_{H2}	—	25	Heat pump	COP_{min}	2.86
Hydrogen vessels	—	15.00	€/kWh_{H2}	—	25		COP_{max}	7

(*continued on next page*)

(*continued*)

Components	Capex			Opex	Lifetime (years)	Components	Efficiency	
	Fixed (€)	Capacity-specific		Fixed + capacity-specific (% inv/a)				
Hydrogenizer	2123.30	761.10	€/kW_{H2}	1.00	20	Thermal storage	$\eta_{ch.\ and\ dis.}$	99%
Dehydrogenizer	1140.00	408.60	€/kW_{H2}	1.00	20		Self-discharge	0.1%h
Low-pressure compressor	—	1716.71	€/kW_p	1.00	25	Electrical heater	η_{el}	98%
High-pressure compressors	560.00	1329.80	€/kW_p	1.00	25	Heat exchanger/Hydrogenation/dehydrogenation	η	99.5%
Heat exchangers 1 and 2	—	1.00	€/kW_{th}	1.00	—	Compressor 2 MPa	η_{el}	94.3%
Expanders 1 and 2	—	1.00	€/kW_{th}	1.00	25	Compressor 16 MPa	η_{el}	95.6%

C. Capacity expansion mathematical formulation [9,71]

The three case studies are modeled using the capacity expansion optimization equations below. The objective function Eq. (6) minimizes the total annual cost of the system consisting of capital expenditures and fixed operational expenditure of the system. Eq. (7) balances the commodities (electricity, heat, and hydrogen). The source, sink, and converters have flow connections with Eqs. (8), (9), and (10). Eqs. (11) and (14) represent the storage flow and the state of charge of the storage respectively, while Eqs. (12), (13), and (15) defines the operational bounds of the components.

Abbreviation	Meaning
M^y	Subsets of the components, at which y can be sources, sinks, converters (conv), storage (store), and commodities (g)
T	Amount of required time steps
x^{op}	Operation rate variable, which extends to charge (ch) and discharge (dis) as in storage
x^{SOC}	State of charge variable
x^{cap}	Installed capacity variable
C^{CAPEX}	Capital expenditures
C^{OP}	Operational expenditures
γ	Conversion factor
η	Efficiency

$$\min\left(\sum_{c}\left(C_c^{capex}+\sum_{t}C_{c,t}^{op}x_{c,t}^{op}\right)\right)\forall c\in M,\ t\in T \tag{6}$$

$$\sum f_{c,t}=0\ \forall c\in M^g,\ t\in T \tag{7}$$

$$f_{c,t}=x_{c,t}^{op}\ \forall c\in M^{source}\cap M^g,\ t\in T \tag{8}$$

$$f_{c,t}=-x_{c,t}^{op}\ \forall c\in M^{sink}\cap M^g,\ t\in T \tag{9}$$

$$f_{c,t}=\gamma_{c,t}x_{c,t}^{op}\ \forall c\in M^{conv}\cap M^g,\ t\in T \tag{10}$$

$$f_{c,t}=x_{c,t}^{op,dis}-x_{c,t}^{op,ch}\ \forall c\in M^{store}\cap M^g,\ t\in T \tag{11}$$

$$x_{c,t}^{op}\geq 0\ \forall c\in M^{source,sink,conv,store},\ t\in T \tag{12}$$

$$x_{c,t}^{op}\leq x_c^{cap}\ \forall c\in M^{source,sink,conv},\ t\in T \tag{13}$$

$$x_{c,t+1}^{SOC}=x_{c,t}^{SOC}+\eta_{c,t}^{ch}x_{c,t}^{op,ch}-\frac{x_{c,t}^{op,dis}}{\eta_{c,t}^{dis}}\forall c\in M^{store},\ t\in T \tag{14}$$

$$0\leq x_{c,t}^{SOC}\leq x_c^{cap}\forall c\in M^{store},\ t\in T \tag{15}$$

D. Sensitivity analysis

Table 5
Results of the minute and hourly resolutions for MG2Lab in terms of the total annualized cost and the associated computational runtime (in brackets).

	Offgrid	Grid
Fully resolved in one minute	22545.06 € (25811.59 sec)	19166.3 € (18336.01 sec)
Averaged one hour resolution	22461.65 € (28.56 sec)	19117.41 € (21.59 sec)

Table 6
Results of the aggregation methods for MG2Lab in terms of the total annualized cost and the associated computational runtime (in brackets).

	Typical days			Typical weeks	
	Offgrid	Grid		Offgrid	Grid
1 × 24	4909.9 € (0.81 sec)	4909.9 € (0.44 sec)	1 × 168	4939.01 € (1.06 sec)	4929.5 € (0.63 sec)
5 × 24	21501.86 € (0.78 sec)	18131.62 € (0.90 sec)	4 × 168	21543.83 € (1.68 sec)	18159.9 € (1.49 sec)
10 × 24	19649.67 € (1.19 sec)	16892.23 € (1.13 sec)	8 × 168	20650.04 € (1.76 sec)	17612.13 € (2.66 sec)
20 × 24	23864.89 € (1.85 sec)	20186.43 € (1.76 sec)	12 × 168	19526.92 € (2.97 sec)	16823.23 € (4.83 sec)
40 × 24	24037.48 € (3.43 sec)	20384.41 € (2.91 sec)	24 × 168	24474.63 € (15.04 sec)	20654.42 € (24.46 sec)
80 × 24	23840.65 € (5.73 sec)	20410.10 € (5.81 sec)	36 x 168	24166.91 € (27.22 sec)	20465.42 € (30.36 sec)
160 × 24	23061.46 € (9.54 sec)	19764.93 € (12.17 sec)	52 × 168	24077.97 € (63.56 sec)	20516.25 € (42.17 sec)
365 × 24	22525.71 € (31.79 sec)	19163.69 € (39.20 sec)			

Table 7
Total annualized cost for both hour and minute-based resolutions in MG2Lab.

No. of Builings	1	2	3	4	5	6	7	8	9	10	11	12
Hourly (€)	4077	8099	11,336	14,799	18,414	22,461	27,123	30,606	34,457	36,421	38,465	43,916
Minute (€)	4114	8140	11,388	14,855	18,487	22,545	27,217	30,712	34,584	36,552	38,608	44,073
Underestimation (%)	0.91	0.51	0.46	0.38	0.40	0.37	0.35	0.35	0.37	0.36	0.40	0.36

Table 8
Clustering methods analyses for SSB 1, comparing the total annualized cost (TAC) and the computational runtime in seconds (in brackets).

Data	TAC, € (Runtime, sec)
Fully resolved in one minute	3623.09 € (254273.71 sec)
Averaged one hour resolution	3589.36 € (3991.02 sec)
TD365 (Hierarchical)	3615.20 € (1153.72 sec)
TD365 (K-means)	3615.20 € (2451.60 sec)
TD365 (K-medoids)	3615.20 € (1117.90 sec)

Table 9
Uncertainty analysis of total annualized cost under variations in photovoltaic (PV) capacity and electricity demand. Results are shown for hourly- and minute-resolutions. Underestimation (%) indicates the ratio of hourly to minute-level cost estimates. The TD365 (hierarchical) case is included for comparison.

Sensitivity Analysis	0.95PV 0.9Demand	0.95PV 1.1Demand	0.95PV Demand	PV 0.9Demand	PV 1.1Demand	PV 1.05Demand
Hourly (€)	3374.82	3878.92	3626.87	3341.06	3837.67	3713.51
Minute (€)	3405.35	3916.24	3660.79	3371.42	3874.77	3748.93
Underestimation (%)	0.905	0.962	0.935	0.909	0.967	0.954
TD365 (€) (Hierarchical)	3398.25	3907.56	3652.91	3364.31	3866.08	3740.64

E. Sampling results

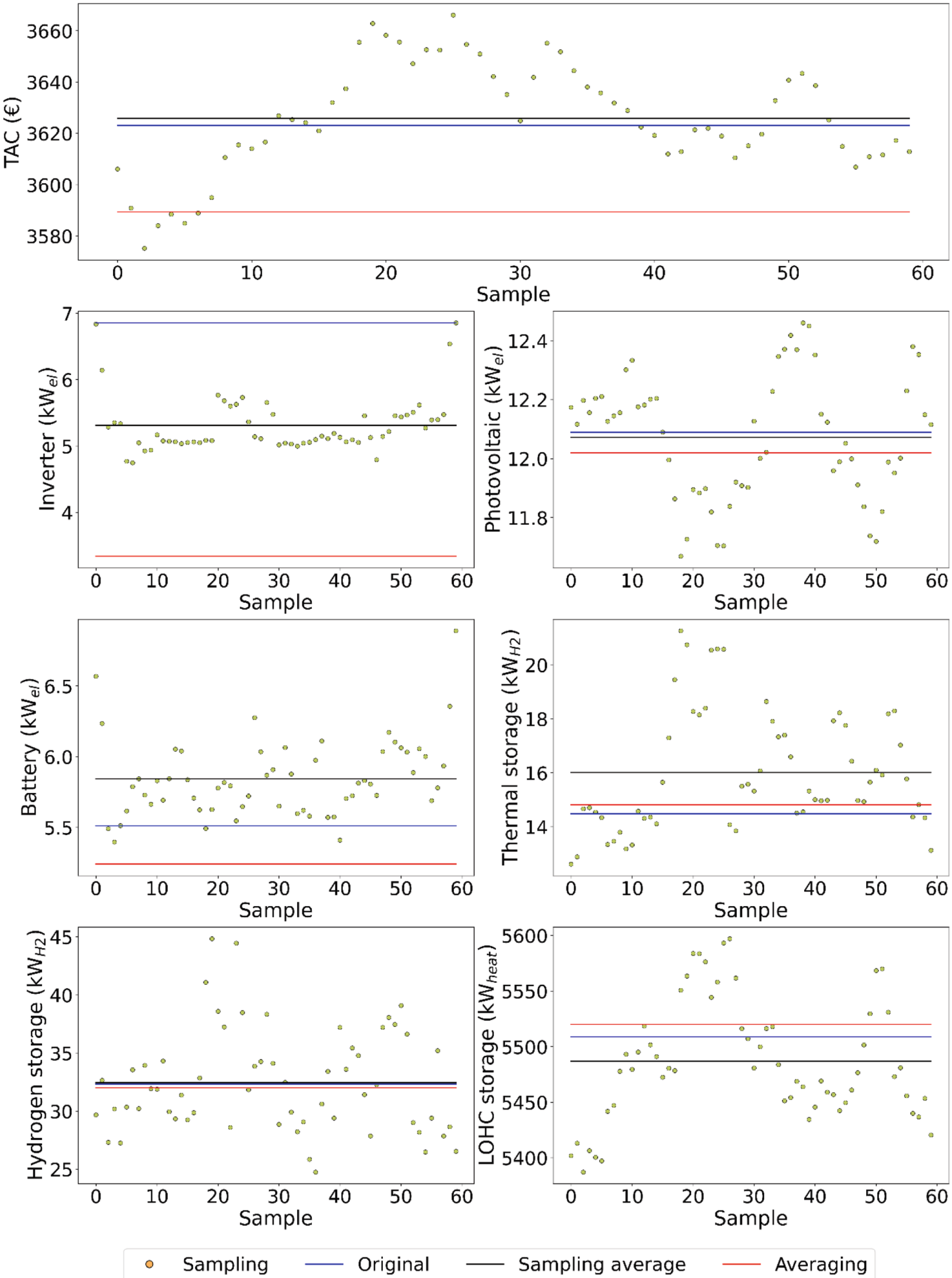

Fig. 17. Total annual cost (TAC) for the sampled data (sampling), original or fully resolved minute data (original), average of the sampled result, and the averaging of the data for SSB 1.

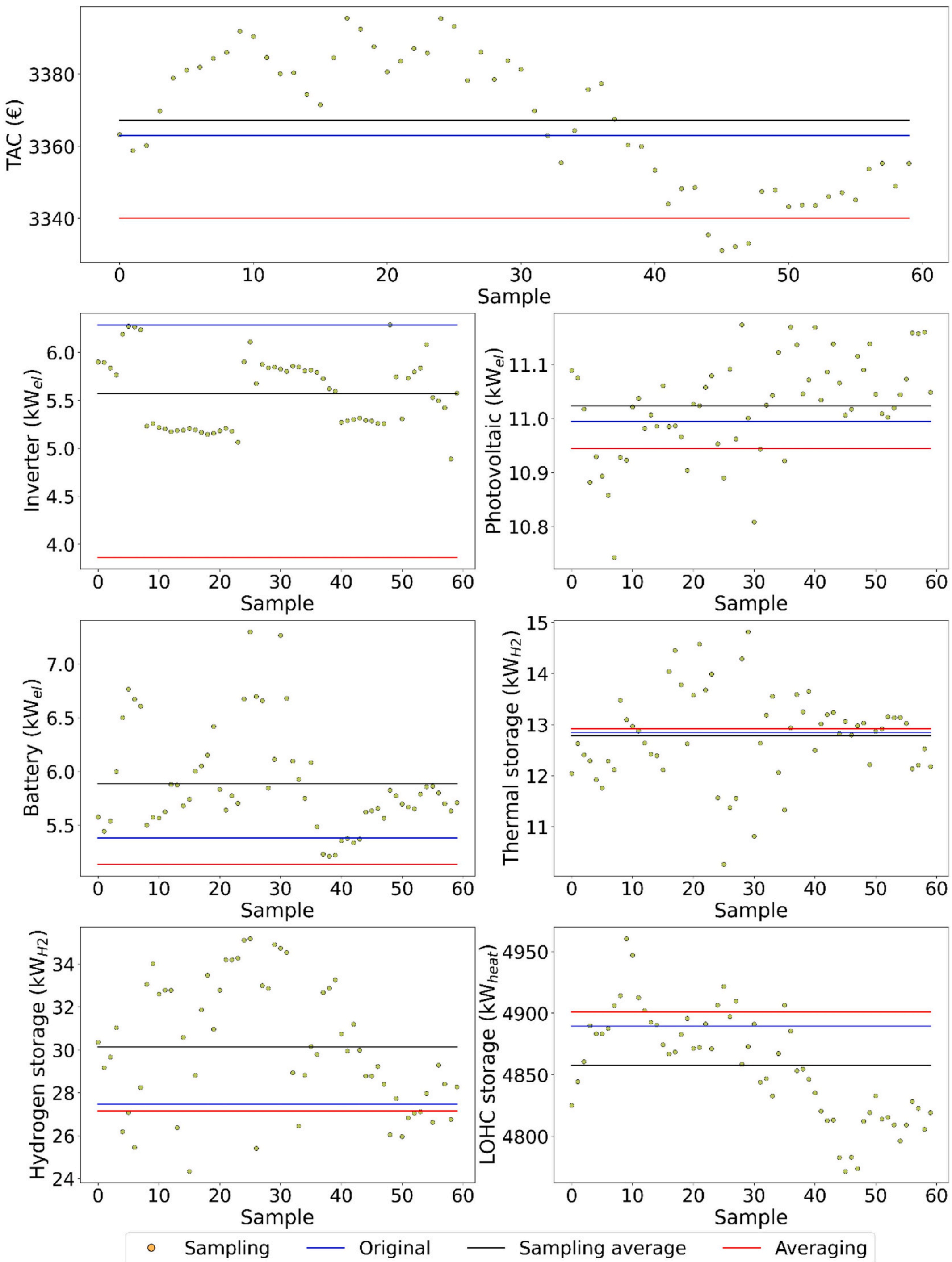

Fig. 18. Total annual cost (TAC) for the sampled data (sampling), original or fully resolved minute data (original), average of the sampled result, and the averaging of the data for SSB 2.

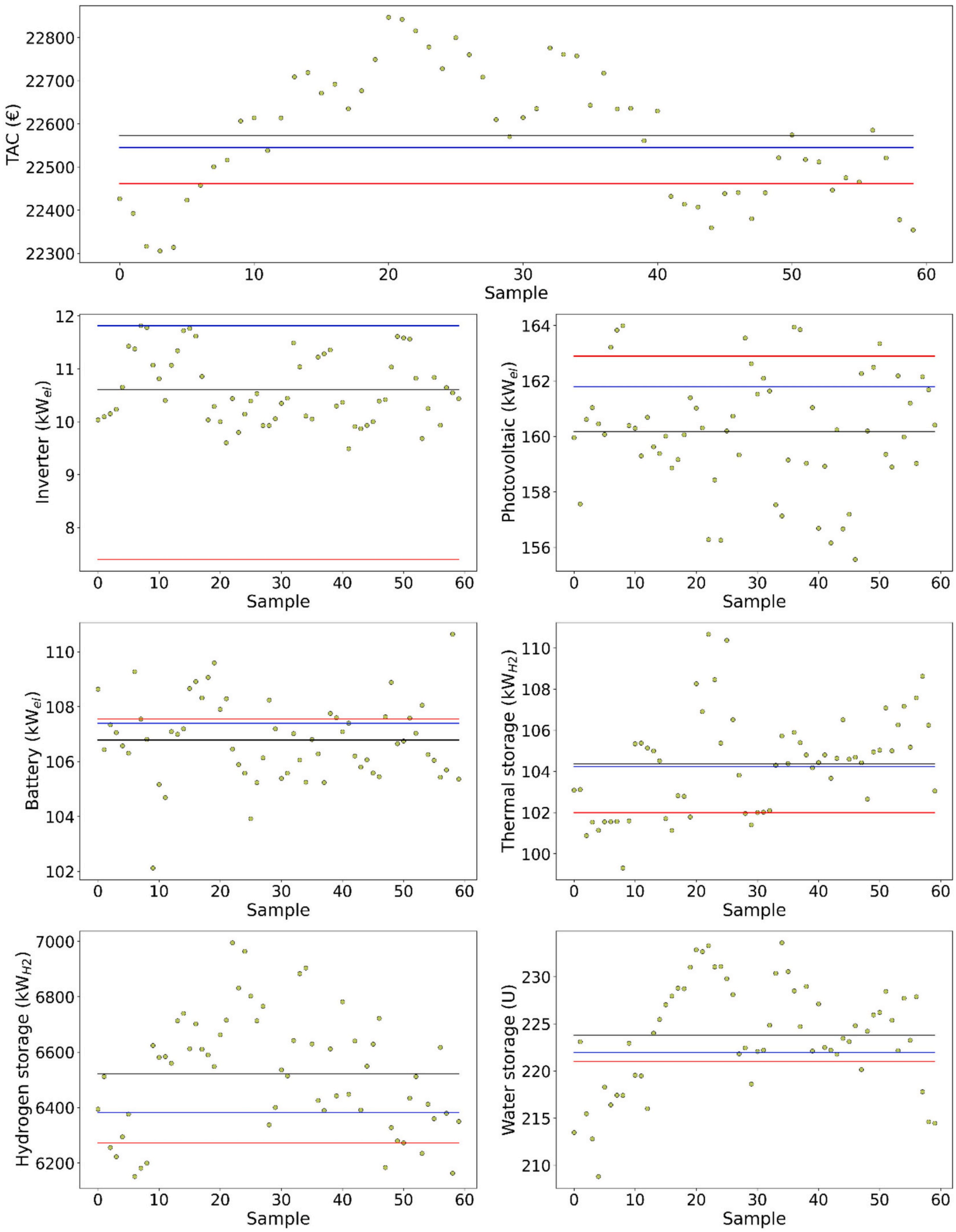

Fig. 19. Total annual cost (TAC) for the sampled data (sampling), original or fully resolved minute data (original), average of the sampled result, and the averaging of the data for MG2Lab.

Data availability

Data will be made available on request.

References

[1] Farghali M, Osman AI, Chen Z, Abdelhaleem A, Ihara I, Mohamed IMA, et al. Social, environmental, and economic consequences of integrating renewable energies in the electricity sector: a review. Environ Chem Lett 2023;21:1381–418. https://doi.org/10.1007/s10311-023-01587-1.

[2] Lund H, Arler F, Østergaard P, Hvelplund F, Connolly D, Mathiesen B, et al. Simulation versus optimisation: theoretical positions in energy system modelling. Energies 2017;10:840. https://doi.org/10.3390/en10070840.

[3] Rauner S, Budzinski M. Holistic energy system modeling combining multi-objective optimization and life cycle assessment. Environ Res Lett 2017;12:124005. https://doi.org/10.1088/1748-9326/aa914d.

[4] Stolten D, Kraus S, Franzmann D, Schöb T, Grube T, Heinrichs H, et al. Neue Ziele auf alten Wegen? Strategien für eine treibhausgasneutrale Energieversorgung bis zum Jahr 2045. Technoökonomische Systemanalyse 2022.

[5] Weinand JM, Hoffmann M, Göpfert J, Terlouw T, Schönau J, Kuckertz P, et al. Global LCOEs of decentralized off-grid renewable energy systems. Renew Sustain Energy Rev 2023;183:113478. https://doi.org/10.1016/j.rser.2023.113478.

[6] Ringkjøb H-K, Haugan PM, Solbrekke IM. A review of modelling tools for energy and electricity systems with large shares of variable renewables. Renew Sustain Energy Rev 2018;96:440–59. https://doi.org/10.1016/j.rser.2018.08.002.

[7] Kiss VM, Hetesi Z, Kiss T. The effect of time resolution on energy system simulation in case of intermittent energies. Renew Sustain Energy Rev 2024;191:114099. https://doi.org/10.1016/j.rser.2023.114099.

[8] Deane JP, Drayton G, Gallachóir BPÓ. The impact of sub-hourly modelling in power systems with significant levels of renewable generation. Appl Energy 2014;113:152–8. https://doi.org/10.1016/j.apenergy.2013.07.027.

[9] Omoyele O, Matrone S, Hoffmann M, Ogliari E, Weinand JM, Leva S, et al. Impact of temporal resolution on the design and reliability of residential energy systems. Energ Buildings 2024;319:114411. https://doi.org/10.1016/j.enbuild.2024.114411.

[10] Pfenninger S. Dealing with multiple decades of hourly wind and PV time series in energy models: a comparison of methods to reduce time resolution and the planning implications of inter-annual variability. Appl Energy 2017;197:1–13. https://doi.org/10.1016/j.apenergy.2017.03.051.

[11] Kazemi M, Siano P, Sarno D, Goudarzi A. Evaluating the impact of sub-hourly unit commitment method on spinning reserve in presence of intermittent generators. Energy 2016;113:338–54. https://doi.org/10.1016/j.energy.2016.07.050.

[12] Omoyele O, Hoffmann M, Koivisto M, Larrañeta M, Weinand JM, Linßen J, et al. Increasing the resolution of solar and wind time series for energy system modeling: a review. Renew Sustain Energy Rev 2024;189:113792. https://doi.org/10.1016/j.rser.2023.113792.

[13] Omoyele O, Belina J, Hartono NTP, Hoffmann M, Weinand JM, Larrañeta M, et al. A python package for temporal downscaling of solar irradiance. SoftwareX 2026;34:102688. https://doi.org/10.1016/j.softx.2026.102688.

[14] B.A. Frew, W.J. Cole, Y. Sun, T.T. Mai, J. Richards, 8760-based method for representing variable generation capacity value in capacity expansion models, National Renewable Energy Lab.(NREL), Golden, CO (United States), 2017. https://www.osti.gov/biblio/1375305 (accessed January 31, 2026).

[15] Thomsen J, Hussein NS, Dolderer A, Kost C. Effect of the foresight horizon on computation time and results using a regional energy systems optimization model. Energies 2021;14:495. https://doi.org/10.3390/en14020495.

[16] Kotzur L, Nolting L, Hoffmann M, Groß T, Smolenko A, Priesmann J, et al. A modeler's guide to handle complexity in energy systems optimization. Adv Appl Energy 2021;4:100063. https://doi.org/10.1016/j.adapen.2021.100063.

[17] Ridha E, Nolting L, Praktiknjo A. Complexity profiles: a large-scale review of energy system models in terms of complexity. Energ Strat Rev 2020;30:100515. https://doi.org/10.1016/j.esr.2020.100515.

[18] Jacobson AF, Mauzerall DL, Jenkins JD. Quantifying the impact of energy system model resolution on siting, cost, reliability, and emissions for electricity generation. Environ Res: Energy 2024;1:035009. https://doi.org/10.1088/2753-3751/ad6d6f.

[19] Marcy C, Goforth T, Nock D, Brown M. Comparison of temporal resolution selection approaches in energy systems models. Energy 2022;251:123969. https://doi.org/10.1016/j.energy.2022.123969.

[20] Bistline JET. The importance of temporal resolution in modeling deep decarbonization of the electric power sector. Environ Res Lett 2021;16:084005. https://doi.org/10.1088/1748-9326/ac10df.

[21] Ernst M, Gooday J. Methodology for generating high time resolution typical meteorological year data for accurate photovoltaic energy yield modelling. Sol Energy 2019;189:299–306. https://doi.org/10.1016/j.solener.2019.07.069.

[22] Mayer MJ. Effects of the meteorological data resolution and aggregation on the optimal design of photovoltaic power plants. Energ Conver Manage 2021;241:114313. https://doi.org/10.1016/j.enconman.2021.114313.

[23] Buchholz S, Gamst M, Pisinger D. Sensitivity analysis of time aggregation techniques applied to capacity expansion energy system models. Appl Energy 2020;269:114938. https://doi.org/10.1016/j.apenergy.2020.114938.

[24] Hoffmann M, Kotzur L, Stolten D, Robinius M. A review on time series aggregation methods for energy system models. Energies 2020;13:641. https://doi.org/10.3390/en13030641.

[25] Wogrin S. Time series aggregation for optimization: one-size-fits-all? IEEE Trans Smart Grid 2023;14:2489–92. https://doi.org/10.1109/TSG.2023.3242467.

[26] M. Hoffmann, Temporal aggregation methods for energy system modeling, (2023).

[27] Gangammanavar H, Sen S, Zavala VM. Stochastic optimization of sub-hourly economic dispatch with wind energy. IEEE Trans Power Syst 2016;31:949–59. https://doi.org/10.1109/TPWRS.2015.2410301.

[28] Lopez ID, Flynn D, Desmartin M, Saguan M, Hinchliffe T. Drivers for sub-hourly scheduling in unit commitment models. In: IEEE Power & Energy Society General Meeting (PESGM). Portland, OR: IEEE; 2018. p. 1–5. https://doi.org/10.1109/PESGM.2018.8586262.

[29] Pandzzic H, Dvorkin Y, Wang Y, Qiu T, Kirschen DS. Effect of time resolution on unit commitment decisions in systems with high wind penetration. In: IEEE PES General meeting | Conference & Exposition. National Harbor, MD, USA: IEEE; 2014. p. 1–5. https://doi.org/10.1109/PESGM.2014.6939548.

[30] Villoz A, Wittmer B, Mermoud A, Oliosi M, Bridel-Bertomeu A, Pvsyst SA. A model correcting the effect of sub-hourly irradiance fluctuations on overload clipping losses in hourly simulations. 8th World Conference on Photovoltaic Energy Conversion. 2022.

[31] Esling P, Agon C. Time-series data mining. ACM Comput Surv 2012;45:1–34. https://doi.org/10.1145/2379776.2379788.

[32] Teichgraeber H, Brandt AR. Time-series aggregation for the optimization of energy systems: goals, challenges, approaches, and opportunities. Renew Sustain Energy Rev 2022;157:111984. https://doi.org/10.1016/j.rser.2021.111984.

[33] Zatti M, Gabba M, Freschini M, Rossi M, Gambarotta A, Morini M, et al. k-MILP: a novel clustering approach to select typical and extreme days for multi-energy systems design optimization. Energy 2019;181:1051–63. https://doi.org/10.1016/j.energy.2019.05.044.

[34] J. Mannhardt, L. Kunz, G. Sansavini, Accurately modeling long-term storage with minimum representative hours in large-scale renewable energy systems, (2025). https://doi.org/10.48550/ARXIV.2512.00892.

[35] Neustroev G, Tejada-Arango DA, Morales-Espana G, de Weerdt MM. In: Hull Clustering with Blended Representative Periods for Energy System Optimization Models; 2025. https://doi.org/10.48550/ARXIV.2508.21641.

[36] Klatzer T, Cardona-Vasquez D, Santosuosso L, Wogrin S. In: Towards Exact Temporal Aggregation of Time-Coupled Energy Storage Models via Active Constraint Set Identification and Machine Learning; 2025. https://doi.org/10.48550/ARXIV.2510.14451.

[37] P. Schäfer, A. Ermshaus, U. Leser, ClaSP - Time Series Segmentation, in: Proceedings of the 30th ACM International Conference on Information & Knowledge Management, ACM, Virtual Event Queensland Australia, 2021: pp. 1578–1587. https://doi.org/10.1145/3459637.3482240.

[38] Cardona-Vasquez D, Klatzer T, Klinz B, Wogrin S. Enhancing time series aggregation for power system optimization models: incorporating network and ramping constraints. Electr Pow Syst Res 2024;230:110267. https://doi.org/10.1016/j.epsr.2024.110267.

[39] Kittel M, Hobbie H, Dierstein C. Temporal aggregation of time series to identify typical hourly electricity system states: a systematic assessment of relevant cluster algorithms. Energy 2022;247:123458. https://doi.org/10.1016/j.energy.2022.123458.

[40] Kotzur L, Markewitz P, Robinius M, Stolten D. Impact of different time series aggregation methods on optimal energy system design. Renew Energy 2018;117:474–87. https://doi.org/10.1016/j.renene.2017.10.017.

[41] Teichgraeber H, Küpper LE, Brandt AR. Designing reliable future energy systems by iteratively including extreme periods in time-series aggregation. Appl Energy 2021;304:117696. https://doi.org/10.1016/j.apenergy.2021.117696.

[42] Hoffmann M, Priesmann J, Nolting L, Praktiknjo A, Kotzur L, Stolten D. Typical periods or typical time steps? A multi-model analysis to determine the optimal temporal aggregation for energy system models. Appl Energy 2021;304:117825. https://doi.org/10.1016/j.apenergy.2021.117825.

[43] Kannengießer T, Hoffmann M, Kotzur L, Stenzel P, Schuetz F, Peters K, et al. Reducing computational load for mixed integer linear programming: an example for a district and an island energy system. Energies 2019;12:2825. https://doi.org/10.3390/en12142825.

[44] Singh B, Rehberg O, Groß T, Hoffmann M, Kotzur L, Stolten D. Budget-cut: introduction to a budget based cutting-plane algorithm for capacity expansion models. Optim Lett 2022;16:1373–91. https://doi.org/10.1007/s11590-021-01826-w.

[45] Schröder T, Kuckshinrichs W. Value of lost load: an efficient economic indicator for power supply security? a literature review. Front Energy Res 2015;3. https://doi.org/10.3389/fenrg.2015.00055.

[46] Gorman W. The quest to quantify the value of lost load: a critical review of the economics of power outages. Electr J 2022;35:107187. https://doi.org/10.1016/j.tej.2022.107187.

[47] Klütz T, Knosala K, Behrens J, Maier R, Hoffmann M, Pflugradt N, et al. A framework for integrated energy system assessment. JOSS 2025;10:6274. https://doi.org/10.21105/joss.06274.

[48] Welder L, Ryberg DS, Kotzur L, Grube T, Robinius M, Stolten D. Spatio-temporal optimization of a future energy system for power-to-hydrogen applications in Germany. Energy 2018;158:1130–49. https://doi.org/10.1016/j.energy.2018.05.059.

[49] Risch S, Weinand JM, Schulze K, Vartak S, Kleinebrahm M, Pflugradt N, et al. Scaling energy system optimizations: techno-economic assessment of energy autonomy in 11 000 German municipalities. Energ Conver Manage 2024;309:118422. https://doi.org/10.1016/j.enconman.2024.118422.

[50] Jacob R, Hoffmann M, Weinand JM, Linßen J, Stolten D, Müller M. The future role of thermal energy storage in 100% renewable electricity systems. Renewable Sustainable Energy Transition 2023;4:100059. https://doi.org/10.1016/j.rset.2023.100059.

[51] Weinand JM, Behrens J, Belina J, Benitez A, Burdack A, Chen S, et al. In: Introducing the ETHOS Energy Transformation Pathway Optimization Model Suite; 2026. https://doi.org/10.2139/ssrn.6620927.

[52] Angur Mahmud Jarman, Hierarchical Cluster Analysis: Comparison of Single linkage,Complete linkage, Average linkage and Centroid Linkage Method, (2020). https://doi.org/10.13140/RG.2.2.11388.90240.

[53] Sinaga KP, Yang M-S. Unsupervised K-means clustering algorithm. IEEE Access 2020;8:80716–27. https://doi.org/10.1109/ACCESS.2020.2988796.

[54] Kotzur L, Markewitz P, Robinius M, Stolten D. Time series aggregation for energy system design: modeling seasonal storage. Appl Energy 2018;213:123–35. https://doi.org/10.1016/j.apenergy.2018.01.023.

[55] Fischer D, Wolf T, Scherer J, Wille-Haussmann B. A stochastic bottom-up model for space heating and domestic hot water load profiles for German households. Energ Buildings 2016;124:120–8. https://doi.org/10.1016/j.enbuild.2016.04.069.

[56] Fischer D, Härtl A, Wille-Haussmann B. Model for electric load profiles with high time resolution for German households. Energ Buildings 2015;92:170–9. https://doi.org/10.1016/j.enbuild.2015.01.058.

[57] S. Leva, A. Nespoli, S. Pretto, M. Mussetta, E. Ogliari, Photovoltaic power and weather parameters, (2020). https://doi.org/10.21227/42V0-JZ14.

[58] Kleinebrahm M, Weinand JM, Naber E, McKenna R, Ardone A, Fichtner W. Two million European single-family homes could abandon the grid by 2050. Joule 2023;7:2485–510. https://doi.org/10.1016/j.joule.2023.09.012.

[59] Kotzur L, Markewitz P, Robinius M, Stolten D. Kostenoptimale Versorgungssysteme für ein vollautarkes Einfamilienhaus. Internationale Energiewirtschaftstagung 2017;10:1–14.

[60] Knosala K, Kotzur L, Röben FTC, Stenzel P, Blum L, Robinius M, et al. Hybrid hydrogen home storage for decentralized energy autonomy. Int J Hydrogen Energy 2021;46:21748–63. https://doi.org/10.1016/j.ijhydene.2021.04.036.

[61] Hoffmann M, Kotzur L, Stolten D. The Pareto-optimal temporal aggregation of energy system models. Appl Energy 2022;315:119029. https://doi.org/10.1016/j.apenergy.2022.119029.
[62] Omoyele O, Hoffmann M, Weinand JM, Larrañeta M, Linßen J, Stolten D. A high-resolution downscaling approach for solar irradiance using statistical parameter matching. Renew Energy 2026;256:124551. https://doi.org/10.1016/j.renene.2025.124551.
[63] Mantuano C, Omoyele O, Hoffmann M, Weinand JM, Panella M, Stolten D. Data imputation methods for intermittent renewable energy sources: implications for energy system modeling. Energ Conver Manage 2025;339:119857. https://doi.org/10.1016/j.enconman.2025.119857.
[64] McKenna R. The double-edged sword of decentralized energy autonomy. Energy Policy 2018;113:747–50. https://doi.org/10.1016/j.enpol.2017.11.033.
[65] Weinand JM, McKenna R, Fichtner W. Developing a municipality typology for modelling decentralised energy systems. Util Policy 2019;57:75–96. https://doi.org/10.1016/j.jup.2019.02.003.
[66] Weinand JM, McKenna R, Kleinebrahm M, Mainzer K. Assessing the contribution of simultaneous heat and power generation from geothermal plants in off-grid municipalities. Appl Energy 2019;255:113824. https://doi.org/10.1016/j.apenergy.2019.113824.
[67] Weinand JM, Ried S, Kleinebrahm M, McKenna R, Fichtner W. Identification of potential off-grid municipalities with 100% renewable energy supply for future design of power grids. IEEE Trans Power Syst 2022;37:3321–30. https://doi.org/10.1109/TPWRS.2020.3033747.
[68] Nespoli A, Mussetta M, Ogliari E, Leva S, Fernández-Ramírez L, García-Triviño P. Robust 24 hours ahead forecast in a microgrid: a real case study. Electronics 2019;8:1434. https://doi.org/10.3390/electronics8121434.
[69] Schöb T, Hoffmann M, Kullmann F, Linssen J, Stolten D. Hydrogen and heat storages as flexibility sources for a greenhouse gas-neutral german energy system. In: Proceedings of the 17th International Conference on Energy Economics and Technology; 2023. p. 1–3.
[70] Gøtske EK, Andresen GB, Neumann F, Victoria M. Designing a sector-coupled European energy system robust to 60 years of historical weather data. Nat Commun 2024;15:10680. https://doi.org/10.1038/s41467-024-54853-3.
[71] Hoffmann M, Schyska BU, Bartels J, Pelser T, Behrens J, Wetzel M, et al. A review of mixed-integer linear formulations for framework-based energy system models. Adv Appl Energy 2024;16:100190. https://doi.org/10.1016/j.adapen.2024.100190.